THE EFFECTS OF STORM EVENTS ON CARBON CYCLING FOR THE NOVA SCOTIAN SHELF REGION

by

Jonathan Lemay

Submitted in partial fulfilment of the requirements

for the degree of Master of Science

at

Dalhousie University

Halifax, Nova Scotia

September 2016

DEDICATION PAGE

This thesis is dedicated to my grandfather, Gérard Rioux, who believed in the importance of our oceans

TABLE OF CONTENTS

LIST OF TABLES

LIST OF FIGURES

ABSTRACT

Seasonal changes in carbon cycling over the years have become better understood on the Scotian Shelf, however little is resolved in short term variation. Focusing on the storm event, Hurricane Arthur, July 5th 2014 there is a drop in the partial pressure of CO_2. With the shelf having carbon rich deep water, a reduction of the partial pressure of CO_2 due to mixing went against current understanding. Slightly above the thermocline there is a sustained population of phytoplankton, causing water in the surrounding area to be lower in dissolved inorganic carbon. When wind mixing from storms occurs, low dissolved inorganic carbon water and phytoplankton from the cold intermediate layer move to the surface. At the surface phytoplankton begin to grow more rapidly due to available nutrients and increased light. This growth and low DIC water then reduces the partial pressure of CO_2 for a short period of time until wind speeds slow down reducing mixing of the water column.

LIST OF ABBREVIATIONS USED

Symbol	Description	Unit
pCO_2	Partial pressure of CO_2	µatm
DIC	Dissolved inorganic carbon	µmol kg^{-1}
HL2	Halifax Line 2 Station	No unit
S	Salinity	No unit
T	Temperature	°C
Chl-a	Chlorophyll-a	mg m^{-3}
MLD	Mixed Layer Depth	m
CIL	Cold intermediate layer	No unit

ACKNOWLEDGEMENTS

CHAPTER 1

INTRODUCTION

1.1 Background

Coastal oceans constitute the interface between the land, sea, atmosphere, and sediment. Due to relatively shallow waters, coastal oceans facilitate the immediate interaction between the atmosphere and sediment (e.g. Thomas et al. 2009). Furthermore, coastal oceans receive runoff from land (Chen and Borges, 2009) and are impacted by the open oceans. They are a hot spot for biological production, and they account for a disproportionate amount of global ocean production relative to their surface area (Cai et al. 2003; Borges et al. 2005). Nutrients from rivers, the open oceans (e.g. Thomas et al., 2005), regenerated nutrients, and nutrients from shallow surface sediments fuel primary producers in coastal oceans. As a consequence, coastal seas account for one-fifth to one-third of ocean primary production even though they only account for 8% of the ocean surface area (Walsh, 1991).

Constituting the joint interface of the four compartments: land, ocean, sediment, and atmosphere, coastal oceans experience much higher spatial and temporal variability at various scales (diel, seasonal, and annual) than the open oceans. This results in challenges when it comes to the determination of the processes controlling this variability (Shadwick et al. 2011). Previous time series analyses of inorganic carbon have been performed on the Scotian Shelf and showed large inter-annual variability

(Shadwick et al. 2010, Shadwick et al. 2011, Shadwick and Thomas 2014, Signorini et al. 2013).

Past studies of the Scotian Shelf have focused primarily on monthly, seasonal, and or inter-annual variation of carbon cycling (Shadwick et al. 2010, 2011, Shadwick and Thomas 2014), but these longer term trends are overlain by significant short-term variations (e.g. Vandemark et al. 2011) that to date, have gone relatively unstudied. Previous studies on the impacts of storms on the Scotian Shelf have primarily focused on their effect towards chlorophyll and timing of the phytoplankton bloom (Fuentes-Yaco et al. 2005 and Greenan et al. 2004). The need to understand short-term variation of carbon cycling is important in better understanding and resolving inter-annual variability for future predictions. In the present study, the causes of short-term variation in carbon cycling will be investigated using autonomous moored sensors, satellite data, and in-situ sample collection.

1.2 Oceanographic Setting

The Scotian Shelf is located in the North West (NW) Atlantic Ocean at the boundary between the subtropical and subpolar gyres and extends from the Cabot Strait to the Gulf of Maine (Figure 1). The primary feature on the Scotian Shelf is the Nova Scotia Current, which is mostly derived from the Gulf of St. Lawrence (Dever et al. 2016). Sea surface temperature (SST) on the Scotian Shelf varies significantly over the course of the year, ranging from approximately 0°C during winter to as high as 20°C during the summer months (Figure 2).

2
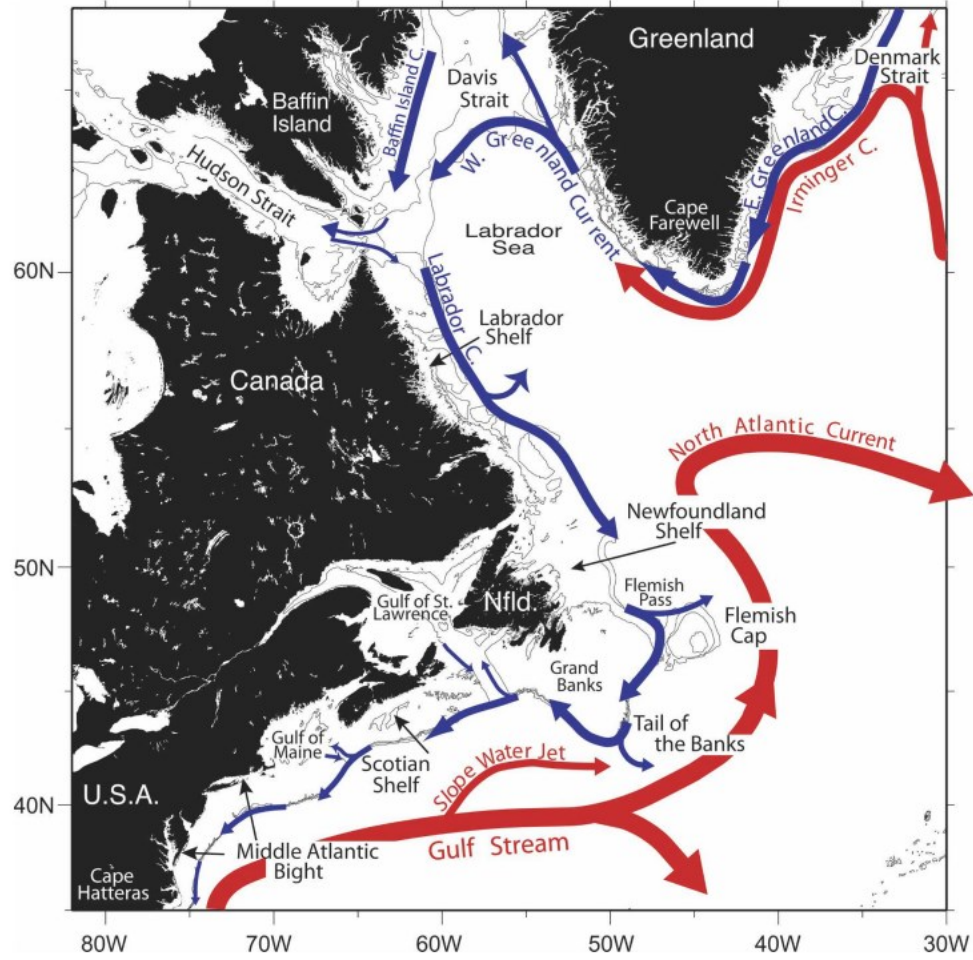
Figure 1: Regional view of the Scotian Shelf with primary currents shown. Photo taken from Fratantoni and Pickart 2007. ©American Meteorological Society. Used with permission.
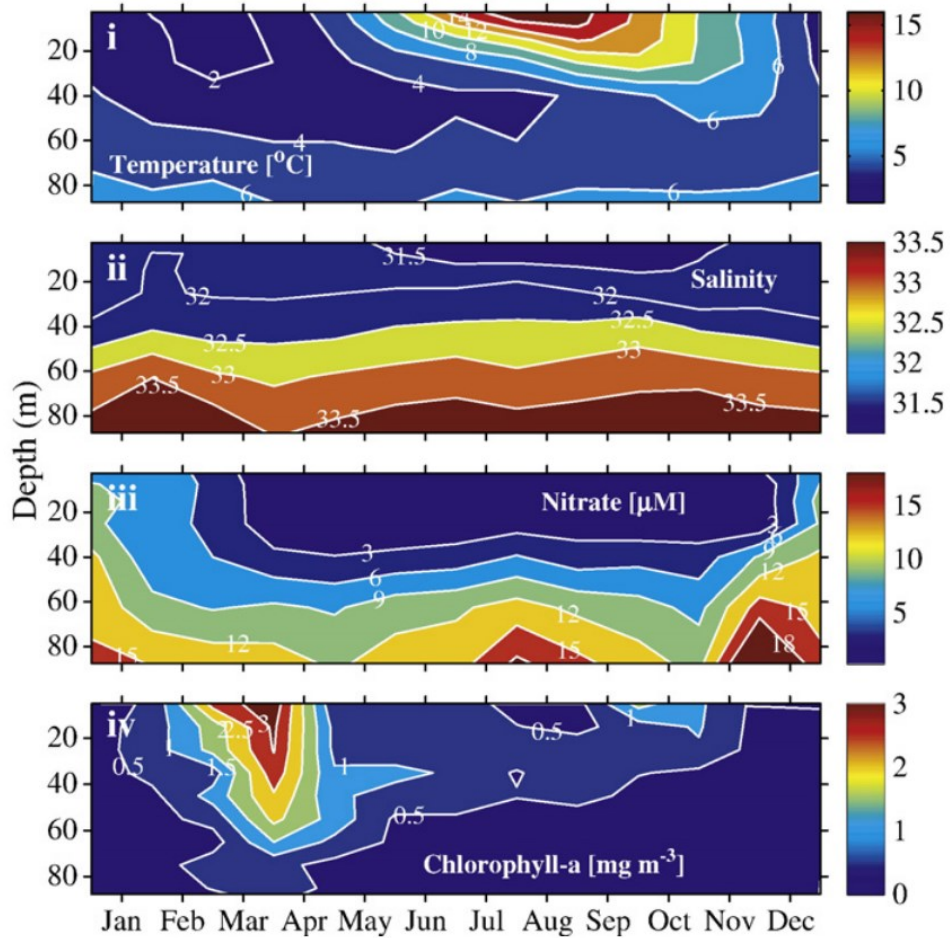
Figure 2: Climatologies for the Scotian Shelf. I) Temperature, II) salinity, III) nitrate, and IV) Chl-a. Reprinted from publication Seasonal variability of dissolved inorganic carbon and surface water pCO_2 in the Scotian Shelf region of the Northwest Atlantic, *Marine Chemesitry* 124:23-37, by Shadwick E.H., Thomas, H., Azetsu-Scott, K., Greenan, B.J.W., Head, E., and Horne, E ©2011 with permission from Elsevier.

Surface salinity in the shelf region is relatively fresh around 30.5 during the winter and 29.5 during late summer when the St. Lawrence river is at peak discharge (Loder et al. 1997, Shadwick et al. 2011, Dever et al. 2016). Salinity increases further off

the shelf as a result of the warm salty water from the Gulf Stream, which bends around the Nova Scotia Current and towards Western Europe.

The MLD is for the Scotian Shelf is deeper in the winter due to stronger winds and convective activity; it is shallower in the summer due to lower wind speeds, warmer surface temperature, and fresh water input (Urrego-Blanco and Sheng 2012, Thomas et al. 2012). The Scotian Shelf can be described as a 2-layer system in the winter, which transitions into a 3-layer system in the summer (Loder et al. 1997). The top layer of the 3-layer system is a warm, shallow fresh water layer; a result of the increased discharge from the St. Lawrence (Loder et al. 1997). To aid in understanding how short term events will impact carbon cycling, a schematic representation of this 2- and 3-layer system is demonstrated in Figure 3. During the winter and early spring the top layer of the 2-layer system contains fresh cold water. During this period the phytoplankton bloom occurs and the mixed layer depth (MLD) begins to shoal rapidly. Once summer is reached, and the outflow from the St. Lawrence is at its peak, the third surface layer forms, which consists of warm fresh water. Below that layer is the cold intermediate layer (CIL), which contains cooler and saltier water. In between the surface layer and the CIL is the temporary sub-surface chlorophyll maximum layer (SCML), a result of the strong stratification between the layers (Cullen 2015). The third layer is the winter mixed layer which contains cooler and saltier water than the cold intermediate layer. When fall approaches, the MLD begins to deepen as a result of decreasing surface temperatures, increased vertical mixing due to higher wind speeds, and decreased outflow of the St. Lawrence. During this period, surface waters begin to cool and increase in salinity until

the system returns to that of panel i) in Figure 3. The MLD on the shelf experiences

variation over the course of the year.

i) Winter / Early Spring **ii) Late Spring / Summer** **iii) Fall / Winter**

Surface

Layer 1-Cooling fresh layer

Layer 1-Warm fresh layer

SCML

Layer 1-Winter mixed layer

Layer 2-Cold intermediate layer

Layer 2-Deep layer

Layer 3-Winter mixed layer

Layer 2-Winter mixed layer

T/S

T/S

T/S

a)

b)

c)

Z

Z

Z
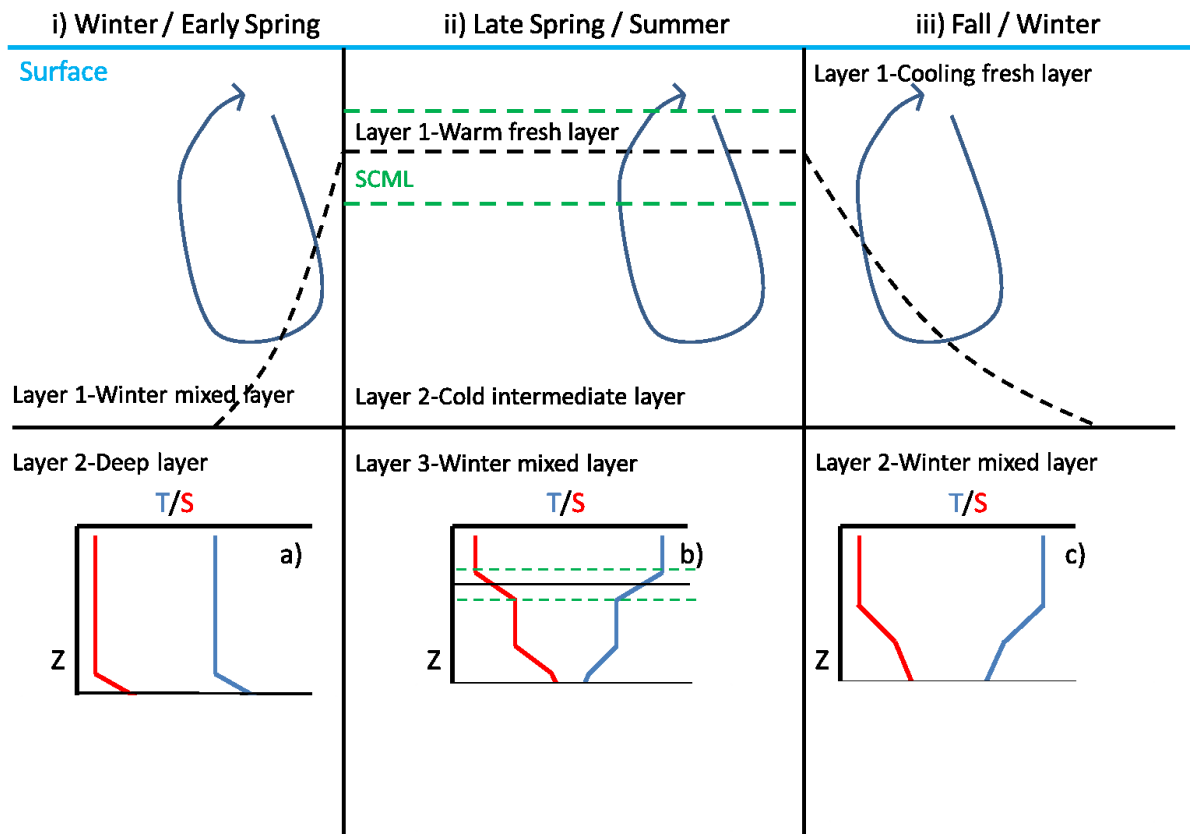
Figure 3: Schematic demonstrating the evolution of the water column over the course of the year. The dashed line intersecting panels i), ii), and iii) represents the mixed layer. SCML in green represents the sub-surface chlorophyll maximum layer. Wind mixing is represented by the circular arrow in panels i), ii), and iii). Temperature and Salinity profiles provide an idealized view of the upper water column where panel a) corresponds to panel i), b) to ii), and c) to iii). The solid lines in panels a), b), and c) represent the location of the borders between the layers in their corresponding i), ii), and iii) panels.

Nitrate on the shelf is heavily influenced by the growth and decay of phytoplankton (Figure 2). During the winter months when wind mixing is at its highest, nitrate levels at the surface are high. As vertical mixing decreases in the spring, phytoplankton begin to grow, quickly depleting the nitrate reservoir in the surface waters. This short but intense bloom heavily influences carbon cycling on the Scotian shelf. During this period the region shifts from being a source of CO_2 to the atmosphere to a sink because of the biological CO_2 drawdown (Shadwick et al. 2010, 2011).

Chlorophyll a concentrations in Figure 2 demonstrate the intensity of the spring bloom during the months of March/April. The timing of the bloom varies between these two months depending on a number of factors including the onset of stratification (Shadwick et al. 2010, Greenan et al. 2004). Once the phytoplankton bloom exhausts nitrate, smaller phytoplankton assemblages take over, as they prosper in lower nutrient environments due to their small size (Craig et al. 2015).

Recent studies on annual observations of pCO_2 clearly reveal the re-occurrence of the significant decrease in pCO_2 caused by the bloom during the early spring months (Shadwick et al. 2011). Prior to and after the bloom there is a winter and summer pCO_2 "baseline" with winter pCO_2 averages lower compared to those observed in the summer.

Subsurface chlorophyll maximum layers (SCMLs) are a feature that is almost ubiquitous when dealing with stratified surface waters (Cullen 2015). The Scotian Shelf has been described as a 2- or 3-layer system with a stratified surface layer (Loder et al.

1997). However, in Figure 2 a SCML is not visible except during the late summer months of July and August. During this period, the surface layer (which is now nutrient poor following the intense growth of the spring bloom) becomes strongly thermally stratified. The phytoplankton, therefore, must migrate to deeper waters where the nutrient concentration is sufficient to support growth, and where they can absorb enough light to drive photosynthesis (e.g. Cullen 2015). This occurs at the nutricline, i.e. the transition from the warm, nutrient poor surface layer to the cooler, comparatively nutrient rich second layer. This process allows phytoplankton to grow below the surface, creating the SCML. Additionally, due to photoacclimation, a survival strategy by phytoplankton in lower light environments, there can be a much larger ratio of chlorophyll to carbon (Chl:C ratio) at the SCML (Cullen 2015). This is a result of phytoplankton increasing their pigment content to increase their ability to absorb more light, and can be erroneously interpreted as an increase in biomass rather than a photoacclimative increase in intracellular chlorophyll concentration (Cullen 2015).

The Scotian Shelf has been found to be a source of CO_2 to the atmosphere, except during the period of the spring bloom (Shadwick et al., 2011). Fluxes of CO_2 to the atmosphere are highly variable outside of the spring bloom period (Shadwick et al., 2010). Wind speeds impact the mixed layer depth, which in turn can impact fluxes on the shelf (Shadwick et al. 2010, Greenan et al. 2008). DIC increases with depth, therefore strong wind events would bring up carbon rich water.

Shadwick et al. (2010, their Fig. 8) demonstrate how weather patterns can have a large impact on monthly variation of CO_2 flux. The strength, timing and frequency of

winter storms can impact the timing of the onset of the spring bloom (Shadwick et al. 2010). The Scotian Shelf has been found to experience periodic storm events (Smith et al. 1978). Spectral analyses have shown that storm events occur at periods of 6 days and 3 weeks (Smith et al. 1978, Shadwick et al. 2010, Thomas et al. 2012).

The Scotian Shelf is impacted by hurricanes, with the 2003 hurricane season generating 14 named hurricanes in the Atlantic Ocean (Fuentes-Yaco et al. 2005). Hurricanes that affect the Western North Atlantic are formed mostly in the Eastern Atlantic Ocean near Africa (Fuentes-Yaco et al. 2005). After formation the hurricanes move westward on the trade winds, veer northeast around 30° to 35°N meeting the eastern prevailing winds from North America, and then at this point the hurricane can pass over the Scotian Shelf and/or the Newfoundland Shelf (Fuentes-Yaco et al. 2005). Hurricanes passing through the northwest Atlantic can entrain cold nutrient rich water to the surface, which has been found to stimulate primary production (Fuentes-Yaco 1997, Platt et al. 2005). The timing of these storms have also been found to affect the timing and strength of the spring phytoplankton bloom (Greenan et al. 2004)

1.3 Objectives

The objective of this thesis is to better understand the mechanisms involved in the high amount of variation associated with pCO_2. This will be accomplished by focusing on one strong storm event. Through this storm event the goal is to develop a better understanding of the relationship between storms and carbon cycling. To

accomplish this objective the study will use high-resolution pCO_2 time series data gathered through autonomous moorings, discrete water samples, and satellite imagery.

CHAPTER 2

Methods

2.1 Sampling Procedures

The CARIOCA buoy used in this study was equipped with sensors to acquire hourly measurements of temperature, conductivity, the partial pressure of CO_2 (pCO_2), salinity, sea surface temperature (SST), and chlorophyll-a fluorescence. An automated spectrophotometric technique was used to estimate pCO_2, and is fully described elsewhere (Bates et al. 2000; Bakker et al., 2001; Bates et al. 2001; Hood and Merlivat, 2001). Conductivity and temperature were measured using a SeaBird conductivity sensor (SBE 41) and a Betatherm thermistor respectively, and a WETstar fluorometer (WETLabs) measured chlorophyll a (Chl-a) fluorescence. The buoy was deployed at the Halifax Line Station 2 (HL2; 44.3N, 63.3W, ~30km offshore from Halifax, Nova Scotia) from February 2014 to January 2015 in addition to other deployments that took place between 2007 and 2012 (e.g., Thomas et al. 2012). A diagram of the placement of the CARIOCA buoy is shown in Figure 4. Data were transmitted daily to the ARGOS satellite system, which was then sent by email and processed through Matlab.

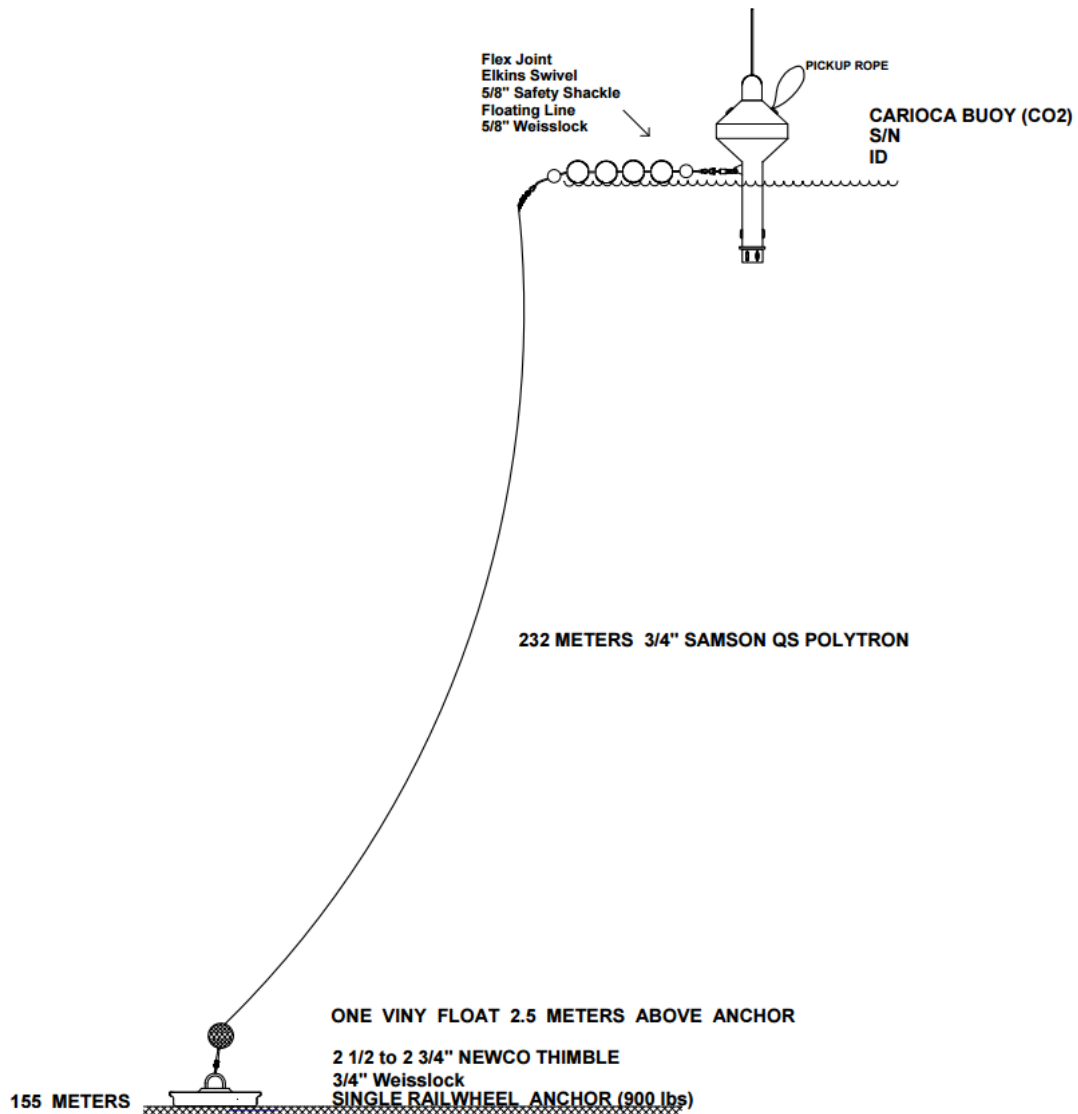**Figure 4:** Schematic of CARIOCA buoy deployed at HL2 station provided by Jay Barthelotte-Bedford Institute of Oceanography/Department of Fisheries and Oceans Canada.

During April to the end of July 2007, a SeaHorse moored vertical profiler was placed at the location of HL2, where it acquired profiles from the surface to a depth of approximately 100 m every 2 hours. It was equipped with temperature, salinity, and Chl-

a fluorescence sensors, and full details regarding the SeaHorse operation and sensor suite can be found in Greenan et al. (2008).

Water column samples were collected through the semi-annual Atlantic Zone Monitoring Program (AZMP). The AZMP cruises occur during the Spring (April) and Fall (September – October) every year. Bi-weekly sampling of HL2 is also conducted whenever weather permits. Water samples are collected using 20 L Niskin bottles mounted on a 24-bottle rosette with a SeaBird CTD. Collected samples are then poisoned with mercury chloride ($HgCl_2$) to prevent biological activity before the pCO_2 concentration was measured using a VINDTA 3C system (Versatile Instrument for the Determination of Titration Alkalinity by Marianda). This was also used to determine alkalinity and DIC, and the measurement method is described in full detail by Johnson et al., 1993, Fransson et al., 2001, or Bates et al., 2005. Certified reference material was provided by G. Dickson (Scripps Institution of Oceanography) to determine the uncertainty of DIC and TA to ±2 and ±3 µmol kg^{-1}, respectively.

2.2 Satellite Data

Satellite data was downloaded and used to make qualitative comparisons with data from the CARIOCA buoy. Surface temperature data was retrieved from the NOAA satellite network database (http://www.esrl.noaa.gov/psd/data/gridded/data.noaa.oisst.v2.highres.html). The range covered is over the Scotian Shelf from July 4th to July 6th 2014. Chl-a surface

concentrations (3 one week averages from June 26th to July 20th 2014), were taken from the GIOVANNI database (http://giovanni.gsfc.nasa.gov/giovanni/).

Non-photochemical quenching (NPQ) in phytoplankton is a mechanism by which excess absorbed solar radiation can be dissipated in pathways (such as heat) other than Chl-a fluorescence, and can reduce chl-a fluorescence by up to 80% (Kiefer, 1973). This was accounted for by using nighttime fluorescence from 0500 UTC for analysis. 0500 UTC was selected for all data analysis in order to minimize the impact of NPQ. Chl-a fluorescence was calibrated to in-situ bottled data to calibrate both the CARIOCA and SeaHorse to the same standard for the purpose of this study.

2.3 Computational Analysis

The data was not normally distributed and had the function log10 + 1 applied. This normalized the data, and had no noticeable effect on the lag function values. Cross correlation lag analyses were performed using R software, and correlation coefficients were found to be statistically significant at the 0.05 level. However, since the maximum temporal resolution of the data was 1-hour, the resolution of the lag times was also 1-hour. This meant that lags between parameters of 1 hour could be subject to significant uncertainty, and it was decided to use only the magnitude of the correlation to identify related parameters and disregard the associated lag period in further analyses.

Temperature mean normalized pCO_2 was calculated using the equation from Takahashi et al. (2002) (Equation1).

$$pCO_2(T^{mean}) = pCO_2^{obs}[\exp(0.0423(T^{mean} - T^{obs}))] \qquad (1)$$

Using this equation removes the thermodynamic effect temperature has on pCO_2 allowing for comparisons between pCO_2 and other variables. The temperature used for this calculation is 10°C.

Using a method developed by Friis et al. (2003), DIC is normalized to salinity to remove the overlying salinity signal to better determine biological and anthropogenic impacts. DIC^S represents DIC adjusted to salinity, S^{obs} represents the measured salinity value, DIC^{obs} represents the measured DIC value, S^{ref} represents the salinity standard used to calculate DIC_s, which in this case is 32, and $DIC^{S=0}$ represents the non-zero freshwater end member, which is 601 µmol kg^{-1} taken from Shadwick et al. 2011.

$$DIC^S = \frac{DIC^{obs} - DIC^{S=0}}{S^{obs}} * S^{ref} - DIC^{S=0} \qquad (2)$$

Sea-air fluxes from the CARIOCA dataset were calculated using the flux calculation functions from Wanninkhof (2014) (Equation 3).

$$F = -0.251 * U^2 * \left(\frac{Sc}{660}\right)^{-0.5} * K_0 * (pCO_2^{Obs} - pCO_2^{Atm}) \qquad (3)$$

Where F is in mol m^{-2} s^{-1}, U is wind speed (m s^{-1}), Sc is the Schmidt number, K_0 is solubility (L^{-1} atm^{-1}), pCO_2^{Obs} (µatm) is observed pCO_2, and pCO_2^{Atm} (µatm) is atmospheric pCO_2 of which 400 µatm is used. Details regarding the flux equation can be found in Wanninkhof (2014).

The hourly observations were used to compute daily averages. Subsequently, the fluxes for each day of the month were averaged together to generate a daily average flux for the month. For the period of Hurricane Arthur (Section 4.2), the daily flux over the 8 days during which the hurricane mixed the water column was averaged. From this 8-day average a monthly average flux was computed to assess the difference between the month with a hurricane and a month long hurricane. This was also the case for the remainder of the month excluding the 8 days of hurricane impact to estimate an expected flux if the hurricane had not impacted the shelf region. The flux calculations from Wanninkhof (2014) have an estimated 20% level of uncertainty. The Wanninkhof method was chosen as it is widely used to calculate pCO_2 fluxes.

A spectral analysis was performed using the Fast Fourier Transform method. The spectral analysis was performed on pCO_2 with the number of values being 7535 and window size of 8000. The frequency range encompassing a 6-day period is plotted to match storm frequencies found in previous work.

2.4 Comparison CARIOCA / SeaHorse

For mechanistic analysis we use the SeaHorse vertical profiler from 2007 to help underpin the observations made from the 2014 CARIOCA dataset. In situ bottled data for chl-a were used to compare nighttime fluorescence from the CARIOCA/SeaHorse data sets (Figure 5). Chlorophyll fluorescence (mg m^{-3} according to the factory calibration values) from both the CARIOCA and SeaHorse were regressed against bottle chlorophyll values to convert to the same chlorophyll standard. r^2 (RMSE) values were found to be

0.532 (0.2 mg m^{-3}) and 0.743 (0.4 mg m^{-3}) for the CARIOCA and SeaHorse respectively. The poor agreement between the bottle and fluorescence Chl-a estimates is unsurprising since factory conversions of fluorescence to chlorophyll concentration rarely correspond well. This is due to several factors that include differences in fluorescence yield between the factory calibration standard and natural phytoplankton, differences in the water mass sampled (small volume illuminated by the fluorometers versus the comparatively larger water mass sampled by the Niskin bottle) and the fact that both estimates are subject to significant uncertainties. For these reasons, fluorescence estimates of Chl-a will be used in a qualitative manner to examine patterns and trends, rather than to determine exact concentrations.

A section of CARIOCA data collected from June 9th-17th (year days 160-168) 2007 to compare with the Seahorse data (Figure 6). The fluorescence for both data sets were converted to chlorophyll using the calibrations curves. Both sets show chlorophyll of similar magnitude, as well as a similar trend over the time series.
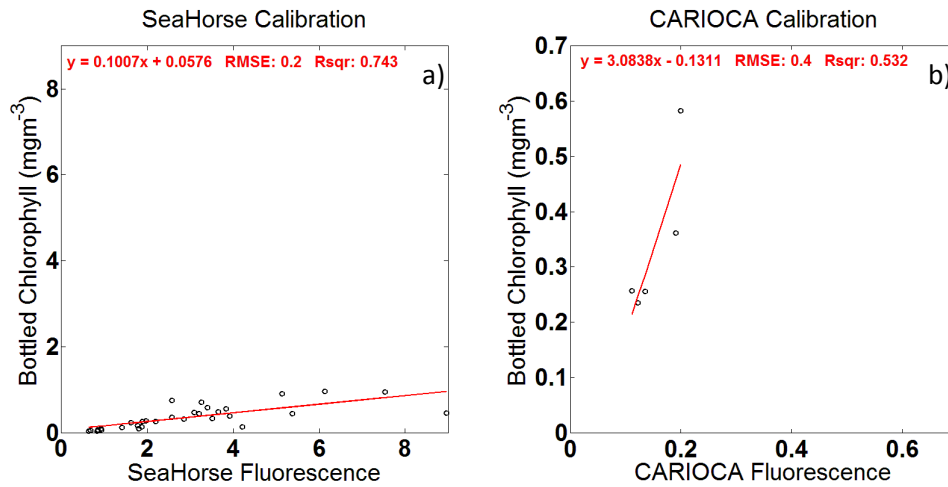
Figure 5: Calibration curves generated from using in-situ bottled chl-a data. Red lines represent the slope with their corresponding equation in the top right. Slope equation, root mean square error (RMSE), and R squared (Rsqr) are at the top of both panels in red.
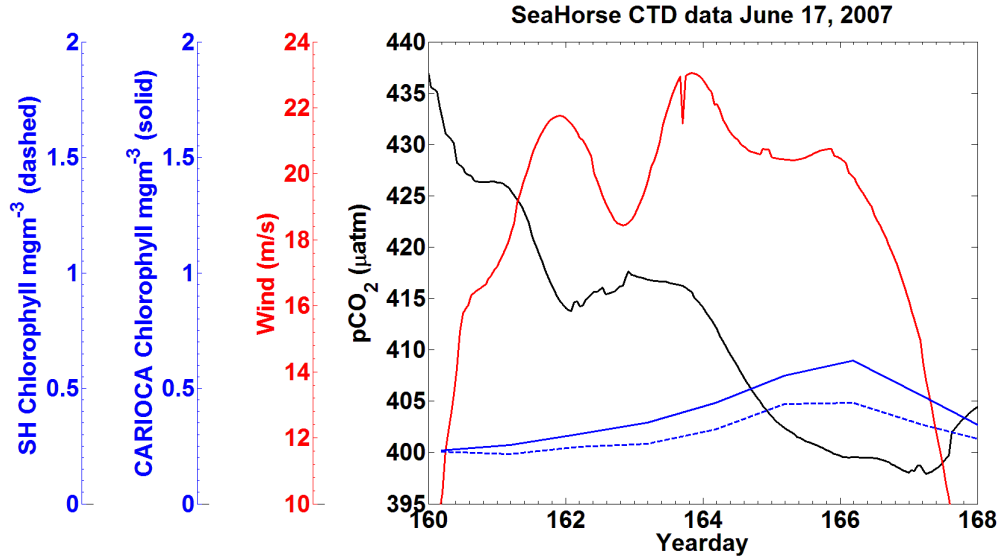
Figure 6: 2007 CARIOCA data set for June 9th-17th from the with the x-axis representing year days. The black line is pCO$_2$ (μatm), red line is wind (m s^{-1}), blue line solid is calibrated CARIOCA fluorescence (mg m^{-3}), and the blue dashed line is calibrated SeaHorse fluorescence (mg m^{-3}).

CHAPTER 3

RESULTS

3.1 Observations of pCO_2, wind speed and fluorescence in 2014

Annual pCO_2 data from the 2014 CARIOCA dataset reveals that there is significant variability over the course of the 2014 year (Figure 7a). Even through the variation, the key annual features still remain; the phytoplankton bloom (year days 80-110), summer baseline (year days 150-300), and winter baseline (year days 50-75 and 300-365). The variability (or amplitude of variability) in pCO_2 is more pronounced during the summer months compared to the winter and the spring bloom (see also Thomas et al., 2012). The low variability during the winter and the bloom is likely a result of the deeper, homogenous surface mixed layer, which in turn acts as buffer for any short-term variability. A spectral analysis of pCO_2 reveals a 5.8 day period (Figure 8), while a spectral analysis of wind showed no significant statistical result. This is an agreement with results from Smith et al. (1978), Shadwick et al. (2010), and Thomas et al. (2012) who found storm periods of around 6 days. To determine the effect this variability has on carbon cycling one event was chosen: Hurricane Arthur. Hurricane Arthur impacted the Scotian Shelf on July 5th 2014 and is marked by the red bars in Figure 5.
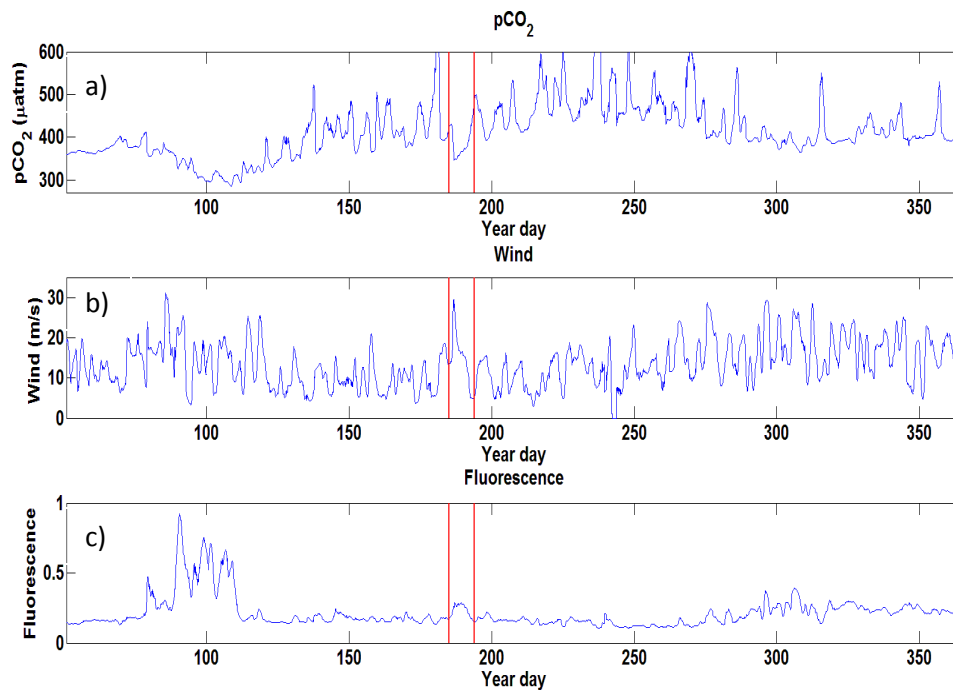
Figure 7: 2014 time series data collected from the CARIOCA buoy with the x axis representing year day. Panel a shows pCO_2 in μatm, revealing a large amount of variation over the course of the year; with a minimum during the spring bloom and a high maximum over the course of the summer. Panel b shows wind speeds in m s^{-1}, with higher wind speeds during the winter period and lower speeds during the summer. Panel c shows fluorescence in arbitrary units with a spring broom clearly visible, and the rest of the year with generally low values. There is some evidence at a prolonged fall bloom after year day 300. The red bands represent the period where Hurricane Arthur (July 5th 2014) took place, and was selected as this feature stands out amongst the others.
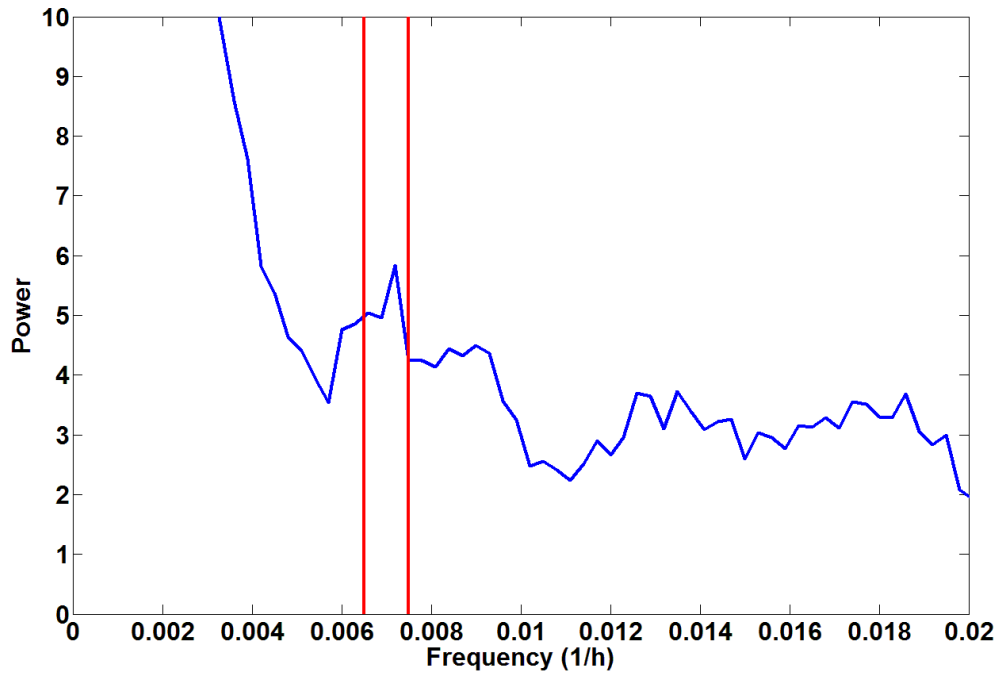
Figure 8: Spectral analysis of pCO_2 from the CARIOCA buoy. Frequency is 1/h where h is hours, and power is in arbitrary units. The red bars represents the frequency range encompassing the 6-day period.

Wind speeds for 2014 (Figure 7b) show that during the winter, winds are stronger on the Scotian Shelf as a result of higher storm frequency and strength; while wind speeds are generally lower during the spring and summer months. During the period of Hurricane Arthur wind speeds were up to 30 m s^{-1}.

Fluorescence over the year (Figure 7c) clearly shows the spring bloom increase of up to a factor of 4 above the winter baseline. During Hurricane Arthur there is a doubling in fluorescence above the summer baseline values compared to the surrounding days. Later in the year, around year day 300, the fluorescence reveals also

somewhat elevated values due to the minor fall bloom that occurs as increased wind speeds begin to deepen the ocean mixed layer bringing nutrients to the surface (Greenan et al. 2004).

3.2 Hurricane Arthur

Satellite data during Hurricane Arthur was used to underpin the data observed by the CARIOCA buoy (Figure 9). Satellite SST and the CARIOCA SST both decrease from about 14.5 °C to 9.5 °C. Chlorophyll estimates from satellite ocean color sensors also indicate a significant increase in phytoplankton during this time, which is in agreement with the CARIOCA observations.

Figure 9: Satellite sea surface temperature data collected from NOAA are shown in panel a (top 4 panels) with a spatial range from 58°W-68°W/40°N-47°N. M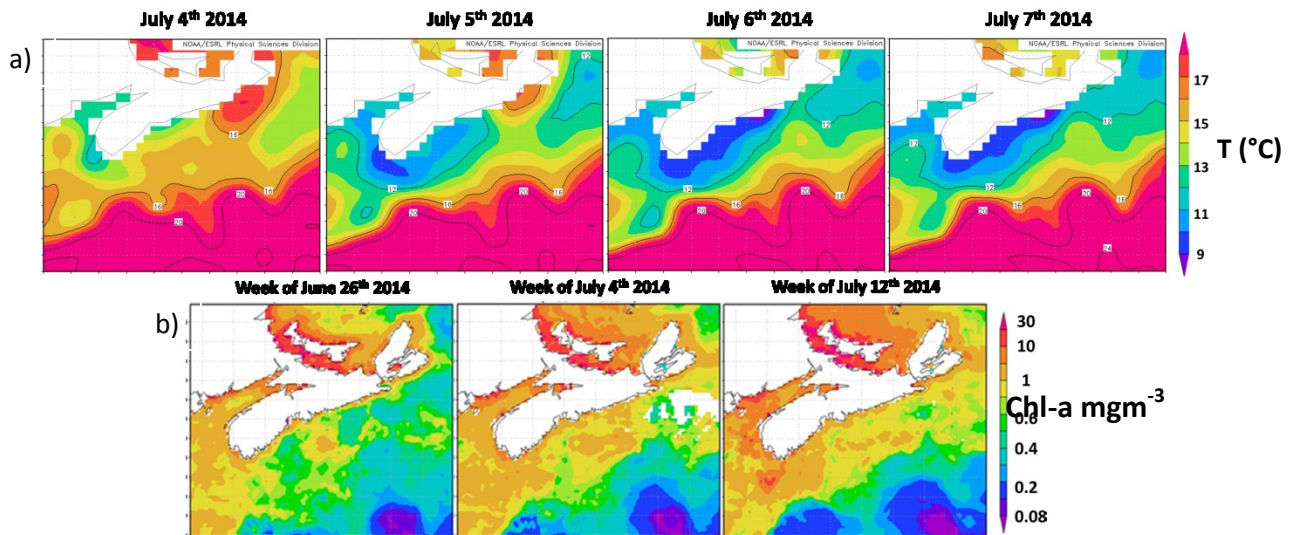ODIS Aqua chl-a data downloaded from GIOVANNI is shown in panel b (bottom 3 panels) with a spatial range of 58.5°W-67°W/40.5°N-47.5°N. The NOAA data shows temperature in °C over 4 days, while the GIOVANNI shows chlorophyll in mgm^{-3} over three time-averaged periods.

One important feature of the time series is that pCO_2 decreases as wind speed increases during the hurricane (Fig 7 days 180-200). Past studies on the Scotian Shelf region have reported that it is primarily a source of CO_2 to the atmosphere (Shadwick et al. 2010). Dissolved inorganic carbon increases with depth in this region (Shadwick et al. 2014), therefore it is expected that increased wind speed would increase pCO_2 as more carbon rich water is brought to the surface. However, the correlation coefficient is -0.77 (not shown) between wind and pCO_2 with a significance level of 0.05 for the whole year. Decreases in pCO_2 with increases in wind are most evident from spring to early fall. This coincides with the period where the water column becomes a 3-layer system as a result of solar insolation and increased discharge from the Gulf of St Lawrence (Loder et al., 1997). For this study we chose the most prominent decrease in pCO_2, which occurred during Hurricane Arthur on July 5th. The assumption is Hurricane Arthur can be compared to other periods where low pCO_2 is the result of high wind events within the spring to early fall period.

In order to identify the cause of the decrease in pCO_2 when wind speeds are high, surface water properties observed during the Hurricane Arthur period are examined in detail (Figure 10). SST drops by roughly 6 °C over a half day period. This indicates that water from the cold intermediate layer (CIL) was mixed into the surface by strong winds (Figure 3). Observations of Hurricane Fabian in 2003 by Fuentes-Yaco et al. (2005) also revealed a decrease in sea surface temperature after the passage of the hurricane. pCO_2 begins to decline before temperature, indicating that lower pCO_2 waters must lie above the thermocline (Figure 10). Shadwick et al. (2014) have shown

that DIC increases with depth, therefore for pCO_2 to decrease before temperature would indicate a mass of relatively poor carbon containing water within the CIL.
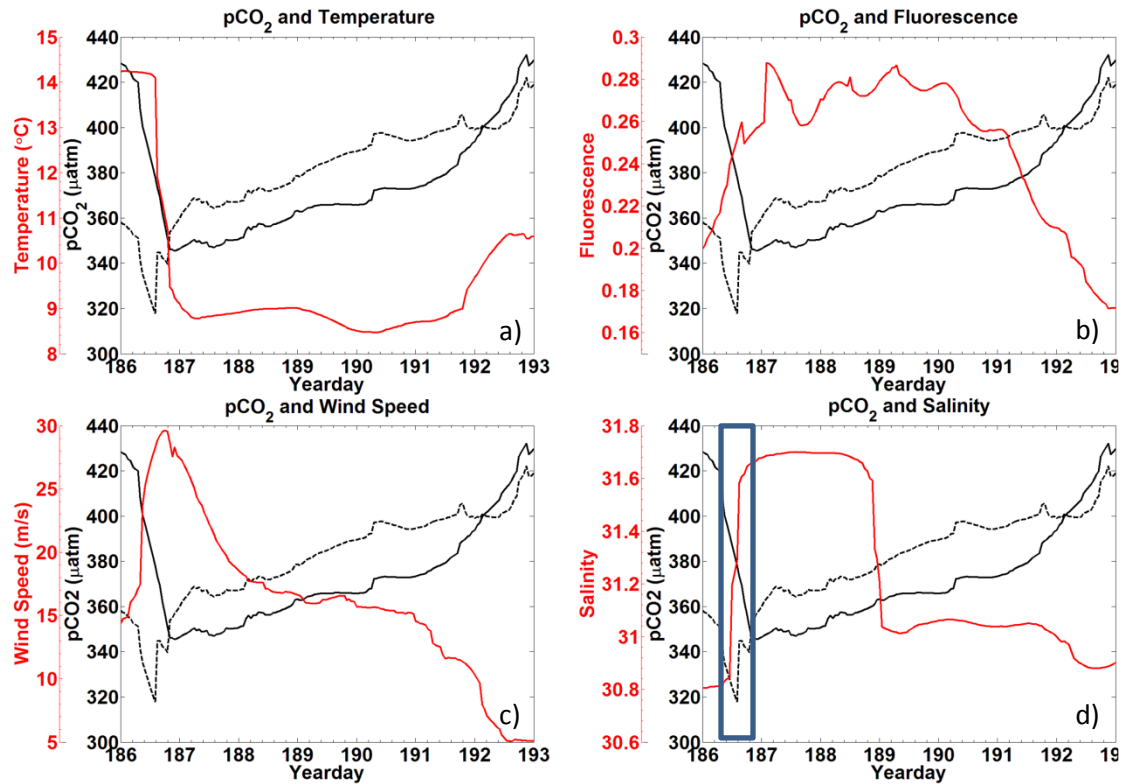
Figure 10: Climatologies for Hurricane Arthur taken from the CARIOCA 2014 dataset, with the x axis again representing year days. Each panel has pCO_2 in black (μatm), with a different variable in each panel overlaid in red. The dashed black line represents the temperature mean normalized pCO_2 (μatm). The blue bar in panel 4 is used to highlight a change in salinity.

Normalizing the DIC water column observations from HL2 to a constant salinity (32) reveals the biological DIC fingerprint (Figure 11b). This approach yields a minimum in DIC in the subsurface layer at a depth of approximately 20-25 m, which indicates DIC uptake by phytoplankton. The layer is enclosed on the top by the fresher surface layer, formed by the outflow of the Gulf of St Lawrence, and on the bottom by the CIL (Figure 3). Further support for the existence of this enclosed layer is provided by a recent study,

Shadwick et al. (2011, their Fig. 13b), in which negative apparent oxygen utilization (AOU) values at this depth level were observed during the summer period. The enclosed layer is both sufficiently shallow for photosynthesis to occur and sufficiently deep to supply the required nutrients through vertical diffusion across the nutricline (Figure 2). When comparing the temperature minimum and salinity maximum from Figure 10 with the T/S profile of Figure 11, they reveal a deepening of the mixed layer to around 25 m, which matches well with the DIC profiles. Figure 11 also shows that the density is stable, and that the DIC minimum lies between low and high density waters.
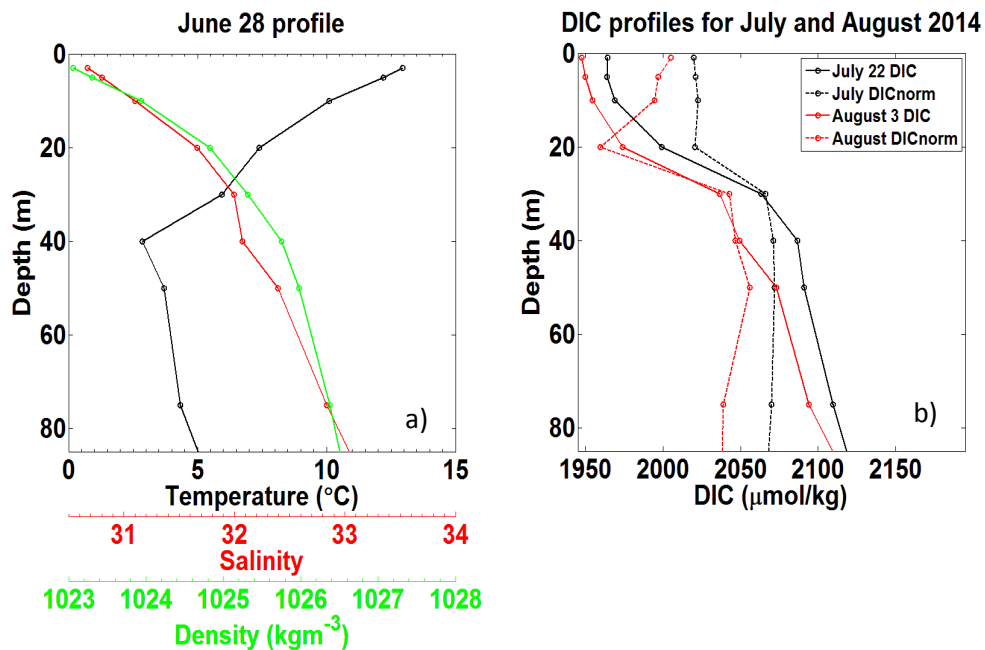
Figure 11: Vertical profiles taken from in-situ samples for HL2. a) salinity, temperature (°C), and density (kg m^{-3}) were collected on June 28th, 7 days before Hurricane Arthur. b) DIC (μmol kg^{-1}) depth (m) profile for July 22 and August 3, 2014 collected at HL2 along with their corresponding profiles normalized to a single salinity value of 32.

In order to shed light on processes occurring within the CIL, we employ high resolution water column data at HL2 collected from the 2007 SeaHorse vertical profiler.

Although the Seahorse data was collected during a different year, we assume that the observed features are present every year as characteristics of the overall system. The data from the SeaHorse profiler shows there is a variable but persistent amount of chlorophyll a below the surface post-spring into summer (Figure 12). This persistent chlorophyll a maximum occurs at roughly 25 m below the surface. This matches well with the profiles in Figure 11 that display DIC minimums at roughly the same depth.
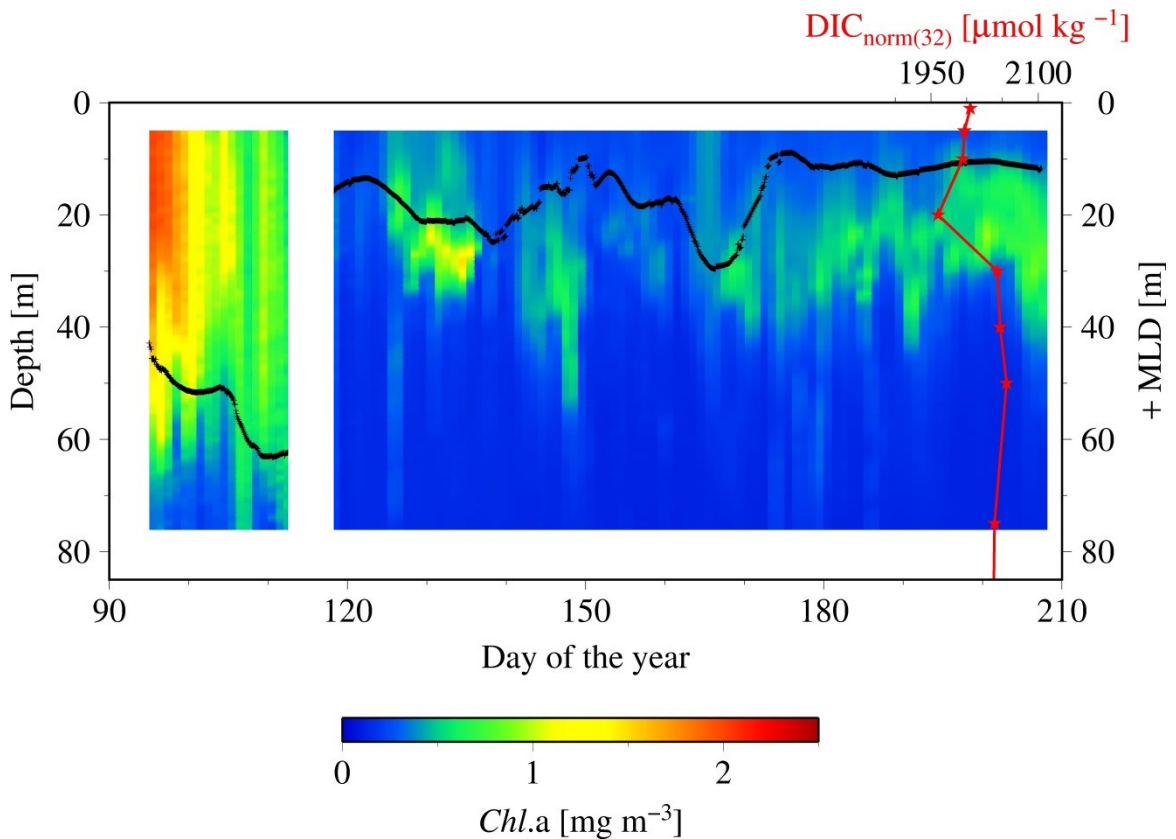
Figure 12: SeaHorse vertical time series data collected at HL2. Fluorescence data is in mg m^{-3} and calibrated to in situ bottle data collected at HL2. White gap represents when the mooring was removed from the water for repairs. The black line represents the mixed layer depth in meters. The red line is a DIC profile from Figure 11, with its scale at the top right of the figure. Please note that the DIC profile is collected from the 2014 year, while the SeaHorse data is from 2007. This comparison is made to help underpin the mechanistic understanding of the water column structure.

With the temperature signal removed by calculating $pCO_2(T_{mean})$, there is a drop in pCO_2 before temperature begins to decline, indicating a non-temperature related impact on pCO_2 (Figure 10). When looking at Figure 3, the decrease in pCO_2 before temperature and sharp decrease in $pCO_2(T_{mean})$ indicates production in the SCML (Figure 3) between the surface layer and CIL. This is supported in Figure 11 where there is a DIC minimum and Figure 12 where there is persistent chlorophyll below the surface. As time progresses after the drop in $pCO_2(T_{mean})$, $pCO_2(T_{mean})$ begins to increase again while temperature remains constant. This is likely a result of the water from the CIL below the SCML being entrained in the mixed layer. When this DIC rich water is brought to the surface it results in an increased pCO_2 concentration. An explanation of the disconnect between temperature and pCO_2 is through the subsurface chlorophyll maximum layer (Cullen 2015). If the chlorophyll maximum begins above the thermocline between the surface layer and the CIL, pCO_2 would drop first as the result of the primary producers being brought to the surface first before the CIL water is entrained and mixed upward. Hurricane Fabian in 2003 also revealed an increase in surface pigment concentrations as a result of the entrainment of nutrient rich waters, stimulating diatom growth; where diatoms have fast growth rates in relatively turbulent waters (Fuentes-Yaco et al. 2005). Also of note is the fast rate at which fluorescence increases. As discussed by Cullen (2015) the SCML contains a higher ratio of chlorophyll to carbon as a result of survival strategy in reduced light (higher intracellular pigment concentration, so they can harvest light more effectively), therefore it is postulated that the rapid increase of fluorescence

could be the result of redistributed cells rather than new production; as cells with high pigment concentration are exposed to light efficiently kicking photosynthesis into action.

A snapshot of SeaHorse profiles from June 9-17th 2007 were extracted and compared to data from the CARIOCA buoy during the same period (Figure 6 methods section). As with Hurricane Arthur, a passing storm (of weaker strength) during this period shows the same negative correlation between pCO_2 and wind speed. pCO_2 decreases for a period of time as wind speeds increase. There is also an increase in chlorophyll for both the CARIOCA and SeaHorse data (Figure 6).

The selected 3 days shown in Figure 13 reveal the evolution of the water column during the 2007 storm event. Before the storm there is a sub-surface chlorophyll maximum, which is below the maximum of the density gradient. Once the storm approaches the water column becomes mixed, increasing surface salinity and chlorophyll as well as homogenizing water density for the top 40 m. In this example however, temperature does not decrease at the surface as in Figure 10. However, Hurricane Arthur was a much stronger storm that resulted in deeper mixing of the water column and more cooling of the SST. When the storm subsides, the water column restores within 2 days to its original state. Surface chlorophyll and salinity return roughly to their pre-storm levels, and the SCML is again below the density gradient.
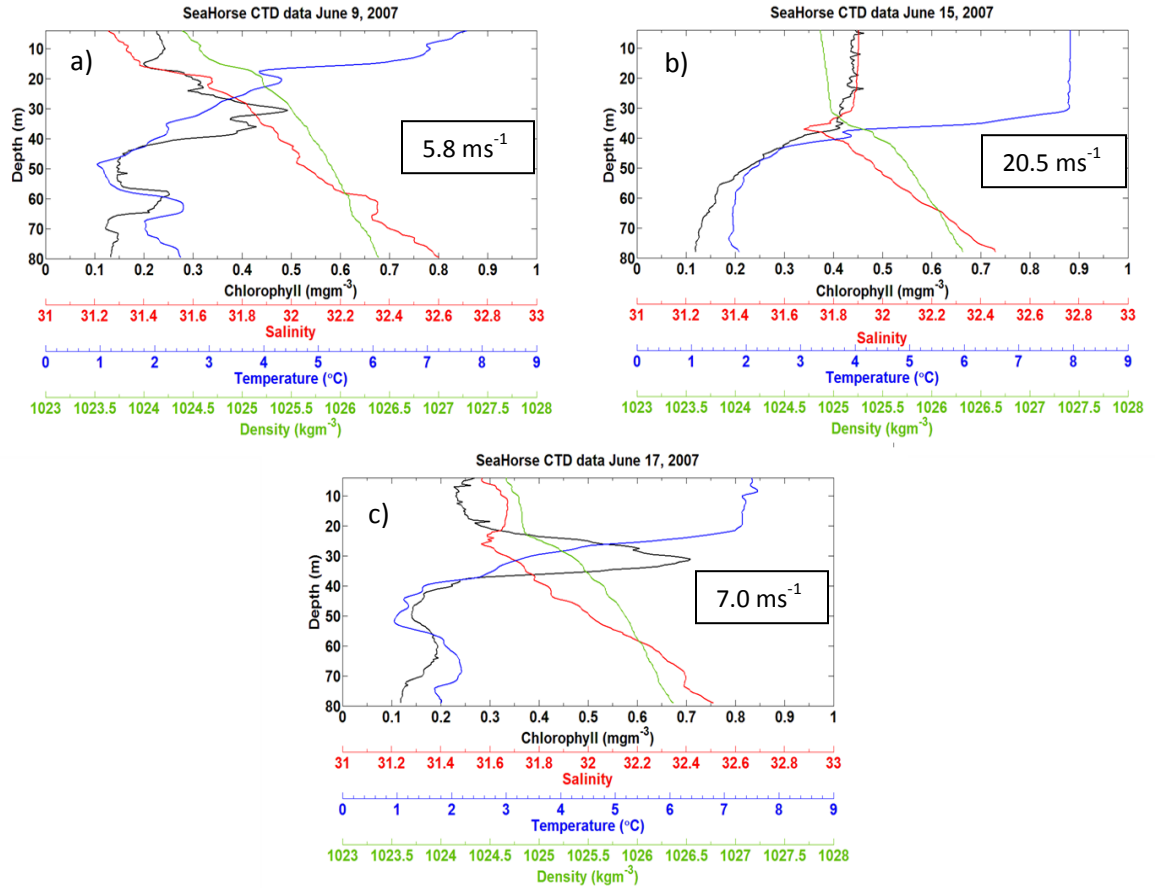
Figure 13: SeaHorse snapshots of a storm event between June 9th to June 17th 2007. X-axis contains chlorophyll (mg m^{-3}), salinity, temperature (°C) and density (kg m^{-3}); and y-axis is depth in metres. Wind speeds (ms^{-1}) for each day (5:00am to correspond with time of SeaHorse data) are included in each panel. Fluorescence values are calibrated to in-situ bottle data collected at HL2.

As discussed by Cullen (2015) the SCML contains a higher ratio of chlorophyll to carbon as a result of survival strategy in reduced light, therefore it is postulated that the rapid increase of fluorescence could be the result of redistributed cells rather than new production. Integrating salinity over a depth of 50 m for June 9th and June 15th in Figure 13 yields a constant salinity inventory of 1474 m and 1482 m respectively. On the assumption that mixing is conservative, integration of chlorophyll a for June 9th and June

15th is also performed. The results were 105 mgChl m^{-2} and 158 mgChl m^{-2} respectively, indicating that the majority of chlorophyll a (approximately 2/3) observed at the surface is redistributed, with the remainder (approximately 1/3) being newly produced. This helps explain the rapid increase in fluorescence observed in Figure 10 as most of the increase is due to redistributed phytoplankton.

Fluorescence during the hurricane doubles, indicating that the mixed conditions of the water column favor phytoplankton growth (Figure 10). Nutrients at the surface are depleted during the summer months (Figure 2) and, therefore, the response of the phytoplankton implies that the hurricane mixed nutrients upward from deeper in the water column; similar to the response of Hurricane Fabian in 2003 (Fuentes-Yaco et al. 2005) and the storm observed in 2007 (Figures 6 and 13). This line of argument is also supported by the observed salinity increase. Looking at Figure 2 and 3, this breaks the fresh water layer at the surface, digging into the deeper saline waters of the CIL; where nitrate is more abundant.

Figure 10 also illustrates the breaking of the enclosed layer in the water column. Between year days 186 and 187 (Figure 10d, blue box), salinity increases in two separate steps. The first step coincides with the sharp decline in $pCO_2(T_{mean})$, indicating the mixing of the phytoplankton-rich enclosed layer to the surface. The second step aligns with the subsequent increase in $pCO_2(T_{mean})$ pointing to continued vertical mixing into deeper saline waters rich in DIC from the CIL. When compared to the wind speeds of Figure 10 in panel c, the second step also occurs during the wind speed maximum, when mixing would be at its strongest. When looking at the 3 layers in Figure 2 during the summer

(dark blue, blue and yellow layers), there is one salinity unit difference between them.

The magnitude of salinity change during Hurricane Arthur is similar.

CHAPTER 4

Discussion

4.1 Impact of Hurricane Arthur on Carbon Cycling

In order to determine the direct impact Hurricane Arthur had on carbon cycling, air-sea fluxes were calculated for the 2014 year (Table 1). The average daily flux for July was 0 mmolC m^{-2} day^{-1}, however when Hurricane Arthur is removed from the average the new flux value is -7 mmol Cm^{-2} day^{-1}. If Hurricane Arthur was averaged alone, the flux would be 19 mmol Cm^{-2} day^{-1}, nearly half the rate of the phytoplankton bloom (45 mmol Cm^{-2} day^{-1}). The impact of the hurricane was substantial enough to cancel out the overall emission of CO_2 to the atmosphere for the month of July. This indicates that short-term storm events can have a significant impact on annual pCO_2 cycling for the Scotian Shelf in the regions affected by the storm.

Table 1: Average daily sea-air fluxes (mmol $m^{-2}day^{-1}$) for each month available for the 2014 year using the Wanninkhof 2014 method. July is broken into 3 components: the month as a whole, the 8 days Hurricane Arthur impacted pCO_2, and the remaining 22 days averaged without hurricane Arthur. pCO_2 (µatm), wind speed (m s^{-1}), temperature (°C), and salinity are averaged for each month (or segment in the case of Arthur and No Arthur).

Month	CO$_2$ Flux (mmol m^{-2}day^{-1})	pCO$_2$ (µatm)	Wind Speed (m s^{-1})	Temperature (°C)	Salinity
March	18	374	14.9	0.1	30.9
April	45	316	14.5	1.2	31.2
May	2	395	9.0	4.5	31.2
June	-3	430	9.1	9.9	30.9
July	0	**423**	**12.2**	**12.6**	**31.1**
Arthur	19	**385**	**14.9**	**9.7**	**31.2**
No Arthur	-7	**436**	**11.2**	**13.6**	**31.0**
August	-27	506	10.8	18.7	30.8
September	-30	481	13.4	17.8	30.8
October	-5	409	17.3	15.0	30.9
November	4	405	17.5	10.3	30.5
December	-8	413	16.3	5.5	30.5

In order to gain a more thorough understanding of how much a hurricane can impact annual carbon fluxes on the Scotian Shelf, a thought experiment was performed. Using methods from Shadwick et al. 2010 (their Figure 4), consisting of breaking the shelf region into 7 box regions (boxes 1-4 along the shelf, 5 and 6 near the Cabot Strait, and

box 7 near the Gulf of Maine), new annual shelf wide fluxes were calculated considering

the impact Hurricane Arthur had on the 2014 year fluxes. Using Figure 9, we determined

what boxes were mainly impacted by Hurricane Arthur. We assumed that boxes 1-4 and

7 are being affected by the hurricane, while boxes 5 and 6 were mainly unaffected. Then

using the flux difference between July (Table 1, the month of Hurricane Arthur) and July

flux where the hurricane signal was removed, new fluxes for each box were calculated

based of Shadwick et al. 2010's annual fluxes (excluding box 5 and 6). This generated a

shelf wide adjustment for the hurricane. This was repeated for all years available in

Shadwick et al. 2010 (Table 2). The new fluxes calculated for each year show a decrease

in annual CO_2 emitted to the atmosphere, with a reversal to uptake in 2006 and 2007.

However, it is important to note that these are very rough estimations and many

assumptions are taken into account. For 2014 there are only 10 available months of data

(January and February the buoy was not deployed). Therefore, the impact of Hurricane

Arthur is larger than it appears as it is being compared to 10 months and not 12.

Secondly, the adjustments to the regional boxes are based on changes located at the site

of the CARIOCA buoy. The shelf is not homogenous (see Signorini et al. 2013), meaning

the level of impact may vary across the shelf compared to the location of the CARIOCA

buoy. Third, the decision of what regional boxes the hurricane impacts are based on

visual observations of data averaged over week periods. Therefore, the regional boxes

affected by Hurricane Arthur are subject to uncertainty. While this thought experiment

does not intend to provide accurate estimations of shelf wide fluxes with the inclusion of

a hurricane, it does show that a single hurricane event can have an impact on the annual

carbon fluxes.

Table 2: Annual fluxes from Shadwick et al. 2010 in mol C m^{-2} yr^{-1} adjusted for the scenario in which Hurricane Arthur would be present those years.

	1999	2000	2001	2002	2003	2004	2005	2006	2007	2008
Shadwick Fluxes	-0.6	-1.3	-0.7	-1.7	-0.8	-1.1	-0.5	-0.02	-0.1	-0.3
Hurricane Arthur Fluxes	-0.4	-1.2	-0.6	-1.6	-0.6	-0.9	-0.3	0.1	0.02	-0.1

4.2 Impacts of storms on other regions

4.1.1 Impacts of other hurricanes in different regions

A study done on the impact of Hurricane Frances in 2004 (first week of

September) that passed along the east coast of the Dominican Republic, Cuba, and then

upwards to Florida showed that decreased surface pCO_2 was primarily the result of

cooler waters brought to the surface (Huang and Imberger 2010). Huang and Imberger

(2010) also found that the passage of Hurricane Frances also caused an efflux of CO_2 to

the atmosphere. The efflux of CO_2 is different than results from Hurricane Arthur. It

was expected for Hurricane Arthur to increase CO_2 emissions to the atmosphere as a

result of deeper carbon rich waters being brought to the surface; however CO_2 fluxes

were lowered as a result of the SCML, which also shows another deviation from results

of Huang and Imberger (2010), where they found temperature to be the primary control

on pCO_2. For the Scotian Shelf the SCML had the strongest impact on pCO_2. An

explanation of why Huang and Imberger (2010) found an emission of CO_2 to the

atmosphere, while Hurricane Arthur showed a decreased emission is the result of the

gradient between the surface ocean and atmospheric pCO_2. Huang and Imberger (2010) had atmospheric pCO_2 values ranging from 335-360 µatm over the course of Hurricane Frances. For Hurricane Arthur an atmospheric concentration of 400 µatm was chosen. Therefore, the gradient from Hurricane Frances compared to Hurricane Arthur was different. Hurricane Frances had surface pCO_2 levels above that of the atmosphere, even though surface pCO_2 decreased from the passage of the hurricane. Where in the case of Hurricane Arthur, surface water pCO_2 went from above 400 µatm before the hurricane, to around 80 µatm below; shifting the gradient direction. As a result Hurricane Arthur had a larger impact on air-sea CO_2 as a result of pCO_2 dropping more substantially than that of Hurricane Frances.

The results from Hurricane Arthur are different than what Bates et al. (1998) who found that the global impact of hurricanes was to emit CO_2 to the atmosphere. The impact of Hurricane Irene (August 2011) on North Carolina's Neuse River Estuary-Pamlico Sound showed the region to go from a carbon sink to a carbon source (Crosswell et al. 2014). Like Hurricane Frances, Hurricane Irene also differs from Hurricane Arthur in that it causes an increased efflux of CO_2 to the atmosphere. Unlike Hurricane Arthur and Frances, pCO_2 at the surface increases for Hurricane Irene as a result of complete water column mixing, with likely sediment re-suspension (Crosswell et al. 2014).

In September 2004 Hurricane Ivan impacted the Gulf of Mexico causing peak concentrations of phytoplankton 3-4 days after Hurricane Ivan passed (Walker et al. 2005). This is similar with Hurricane Arthur where phytoplankton persisted a few days after the Hurricane Arthur's passage (Figure 10).

4.1.2 High frequency observations in other regions

Comparing CARIOCA results from the Scotian Shelf, work from Bates et al. (2001) deployed CARIOCA buoys in the Bermuda coral reef to look at high frequency variation similar to this study. They found that there was a periodicity in fCO_2 (fugacity of CO_2) of 2-8 days. This is similar to the Scotian Shelf where the periodicity was found to be 5.8 days (Figure 8); indicating that their CARIOCA study also revealed high frequency variation in CO_2 as a result of periodic storm events.

A study performed in the Greenland Sea gyre with a deployment of drifting CARIOCA buoys were done by Hood et al. (1999). They found that surface water CO_2 was under saturated with respect to atmospheric CO_2, causing the Greenland Sea gyre to be a sink of CO_2. These observations differ from the Scotian Shelf where surface water CO_2 is oversaturated compared to atmospheric pCO_2 for most of the year, except during the spring bloom (Figure 7).

Another study observing CO_2 with the use of a CARIOCA buoy deployed near Bermuda was performed by Bates and Merlivat (2001), who were looking at short term wind variability on air-sea CO_2 exchange. They found that using high frequency wind data from the CARIOCA buoy, with hourly measurements, better estimate air-sea CO_2 exchange than using wind data measured on timescales of a day or more.

4.3 Impact of other storm events during 2014

With the impact of Hurricane Arthur assessed, the next goal is to determine the impact of other storms on carbon cycling. Three additional storms were briefly assessed with the first being from March 25th to March 29th, during the time of the spring bloom

(Figure 14). Wind speeds were comparable to those of Hurricane Arthur at 30 m s^{-1}, however the impact on pCO_2 was not as significant; decreasing only by 17 µatm compared to Hurricane Arthur's 80 µatm. Fluorescence decreases over the course of this storm, while salinity and temperature increases. $pCO_2(T_{mean})$ also decreases during the peak of this storm. During this time of the year the water column is still a 2 layer system, unlike the 3 layer system observed during Hurricane Arthur. This helps to explain what is being shown with fluorescence, salinity, temperature, and $pCO_2(T_{mean})$. The decrease in fluorescence can be attributed to further deepening of the mixed layer, causing phytoplankton to be mixed down beyond the photic zone. This is shown in Greenan et al. (2004) who found that a down welling event terminated the spring bloom by causing chlorophyll concentrations to be lowered by spreading the phytoplankton over a greater depth and suppressing the nitrate isopleths lowering nutrients in the euphotic zone. There is also the possibility of lateral mixing at the surface as well. Unlike Hurricane Arthur, there is no sharp increase in fluorescence at the start of the storm. This can be explained by the fact that fluorescence at this point in time is high at the surface as a result of the phytoplankton bloom beginning to occur at this time. The increase in temperature and salinity can be explained by breaching the shoaling mixed layer, where more saline and warmer (warm compared to the 0 °C surface water) are brought to the surface (Figure 3). $pCO_2(T_{mean})$ reveals biological drawdown of pCO_2 during the storm. This is shown through the difference in the peak of pCO_2 and its minimum later in the storm. The difference for $pCO_2(T_{mean})$ is around 30 µatm while

pCO$_2$ is 17 µatm.   The 13 µatm of difference can be attributed to the effect of temperature on pCO$_2$.
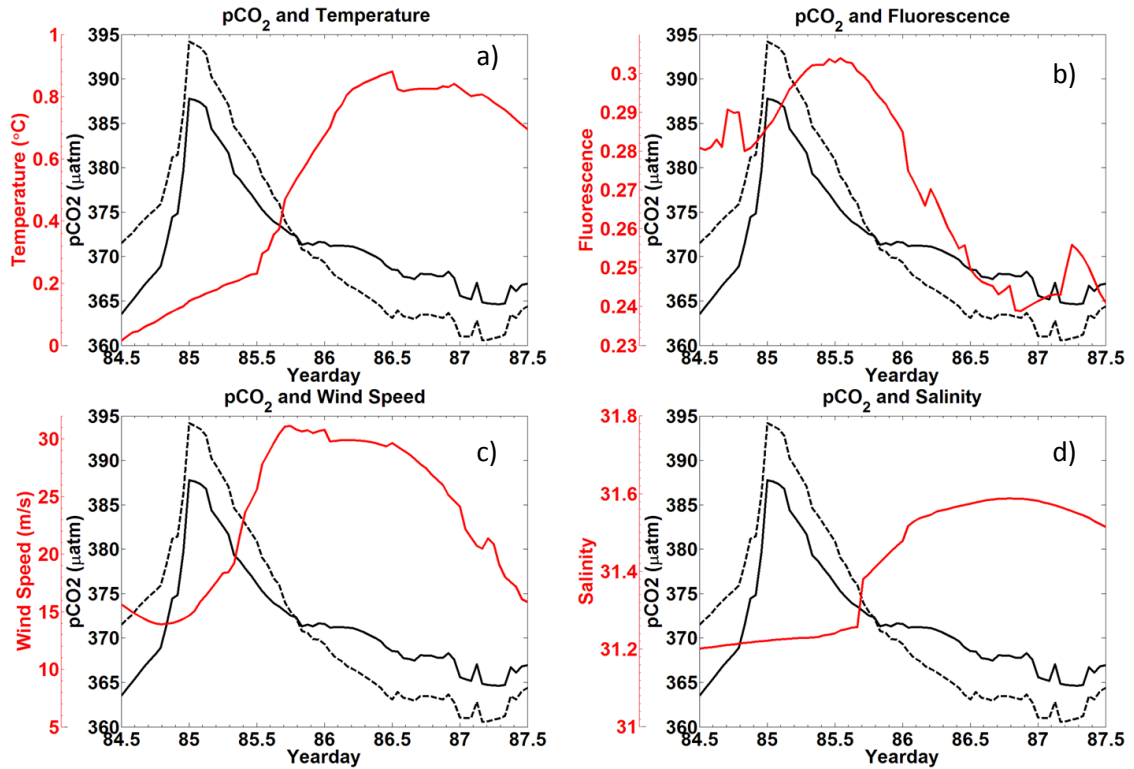

Figure 14: Climatologies for March 25th to March 29th taken from the CARIOCA 2014 dataset, with the x axis representing year days. Each panel has pCO$_2$ in black (µatm), with a different variable in each panel overlaid in red. The dashed black line represents the temperature mean normalized pCO2 (µatm).

Another storm is assessed during the spring from April 22nd to May 2nd (Figure 15). Similar to the storm from March 25th to March 29th, pCO$_2$ only varies around 20 µatm, however this storm's wind speeds are 25 m s^{-1} which are lower than those of Hurricane Arthur which are 30 m s^{-1}. In this storm period there are two storm events back to back, with roughly a day in between both peaks in wind speed. The two spikes in wind speed are followed by increases in pCO$_2$, temperature, and salinity after sustained

wind speeds. Similar to the storm event from March 25th to March 29th, it is assumed

that the shoaling mixed layer is breached bringing up warmer, saline, and more carbon

rich water (Figure 3). Fluorescence also increases rapidly, the result of redistributed cells

(approximately 2/3 from the integration calculation).
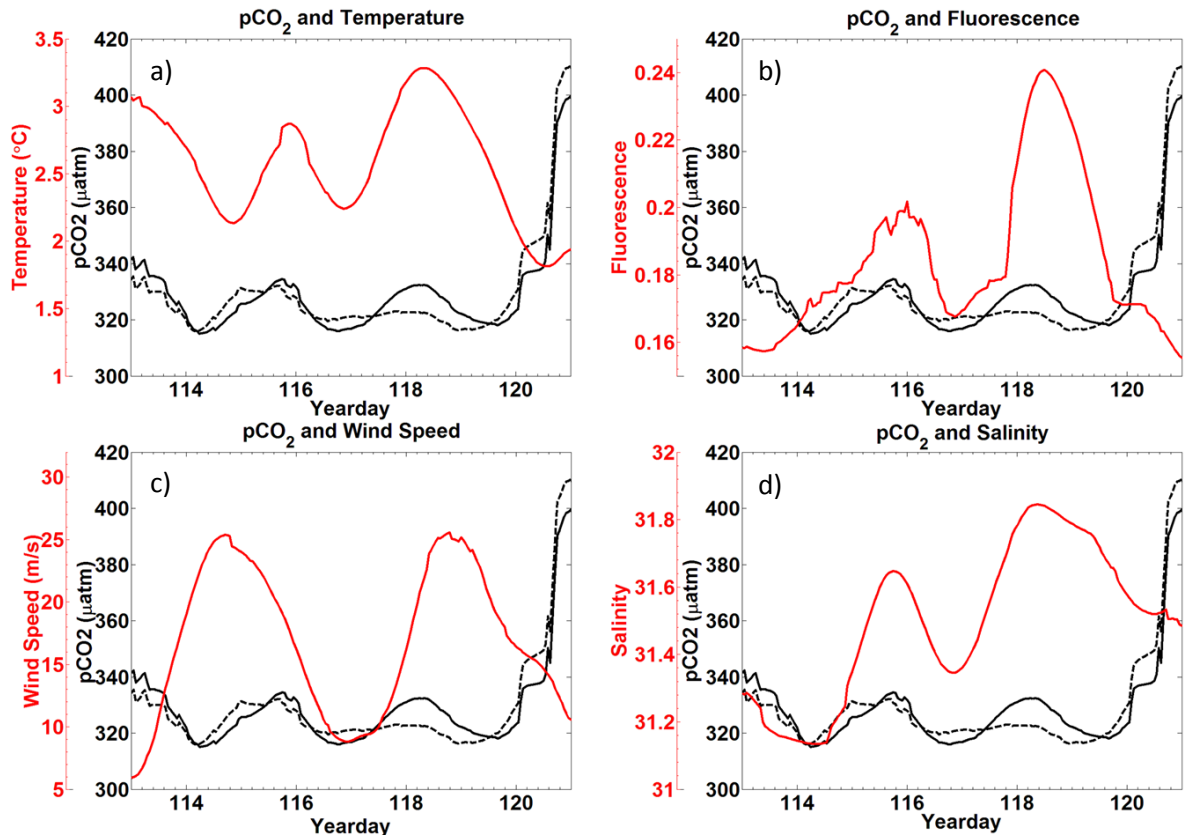
Figure 15: Climatologies for April 22nd to May 2nd taken from the CARIOCA 2014 dataset, with the x axis representing year days. Each panel has pCO_2 in black (µatm), with a different variable in each panel overlaid in red. The dashed black line represents the temperature mean normalized pCO_2 (µatm).

The third and final storm event chosen for analysis was from October 21st to

October 27th during the fall period (Figure 16). Winds speeds for this storm were of

similar magnitude to Hurricane Arthur at 30 m s^{-1}. However, this storm's impact was

more similar to Hurricane Arthur than the two storms from the spring period. pCO_2

dropped by roughly 30 µatm while salinity and fluorescence increased, and temperature

dropped. These trends are the same as those experienced by Hurricane Arthur when the

water column is a 3 layer structure. However, during the fall the water column begins to

return to a 2 layer system as surface temperatures decrease and the outflow of fresh

water from the Gulf of St. Lawrence decreases. This transition is noticeable in the data

for this storm event. Even though wind speeds are similar to those of Hurricane Arthur,

the change in salinity is only an increase of 0.25 compared to 1 unit for Arthur.

Temperatures only drop by 1.4 °C instead 6 °C from Hurricane Arthur.   This is an

indication that the water column is more homogenized due to a deepening of the mixed

layer. One interesting feature was that fluorescence actually increases by nearly 0.2

compared to 0.1 from Arthur, indicating a larger reaction by phytoplankton. There is a

fall bloom during this period, and the increased mixing could be supplying additional

nutrients. Greenan et al. (2004) have also found that storms during this period promote

the fall bloom as a result of bringing nutrients to the surface. The sharp increase in

fluorescence over a short period of time can be attributed to the higher intracellular

pigment concentration. Near the end of the storm fluorescence begins to decrease,

likely an indication of phytoplankton being mixed too deep to receive adequate light for

growth. Temperature also increases during this phase, indicating deeper warmer water

is brought to the surface. The deeper warmer water is a result of the surface layer

beginning to cool during the fall. Similar to Figure 14, $pCO_2(T_{mean})$ shows a larger gap

between peak and maximum than pCO_2. Comparing year day 296 and 298 between

pCO$_2$(T$_{mean}$) and pCO$_2$ reveals a difference of around 40 µatm and 15 µatm respectively. This is a result of biological production masked by the effect of temperature increase. The increase in temperature also indicates deeper mixing, which also brings up carbon rich water. Another possible explanation could also be attributed to lateral transport, as temperature gradient of 2-6 °C are possible along the shelf at the surface (Loder et al. 1997).
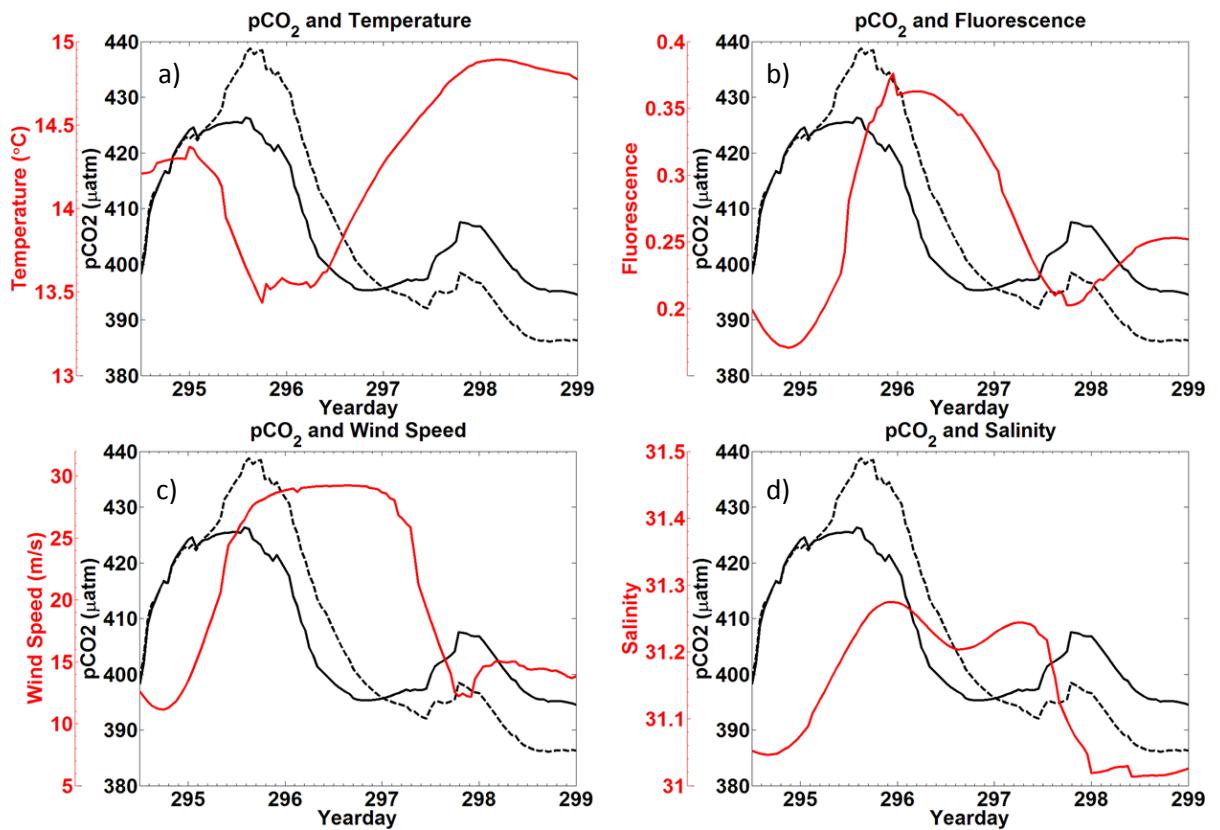

Figure 16: Climatologies for October 21st to October 27th taken from the CARIOCA 2014 dataset, with the x axis representing year days. Each panel has pCO$_2$ in black (µatm), with a different variable in each panel overlaid in red. The dashed black line represents the temperature mean normalized pCO$_2$ (µatm).

4.4 Conclusion

The data provides strong evidence that there is an interaction between wind speed, pCO_2, and sub-surface phytoplankton. However, the timing of a storm event indicates the strength of its impact. Previous work has shown that deeper water is rich in DIC compared to the surface, and it was expected that mixing of deeper water should increase pCO_2 as a result. However, sub-surface phytoplankton has a relatively strong influence on carbon cycling during storm events. The effects of storms on pCO_2 vary based on whether the water column is a 2- or 3-layer system; and their timing during these 2- and 3-layer periods. Hurricane Arthur was a special case in that it impacted the shelf while it was a 3-layer system. During this time the entrained layer was stable as a result of the warm freshwater cap at the surface (Figure 17). This allowed for phytoplankton to thrive between the surface layer and the CIL. When the storm arrived and perturbed this enclosed layer it caused a sharp growth in phytoplankton, which has been seen in other storm events (Greenan et al. 2004 and Fuentes-Yaco et al. 2005). However, due to the timing of Hurricane Arthur during the 3-layer system the effect was more pronounced. The other storms observed in Figures 14, 15, and 16 showed weaker effects which is likely a result of the enclosed layer moving with the MLD and not being as stable as the one found during Hurricane Arthur in the 3-layer system. Compared to other hurricanes (Huang and Imberger 2010 and Crosswell et al. 2014), Hurricane Arthur had a different impact in that it pushed the shelf towards a sink of CO_2. The hope is that this research will help aid in the general knowledge of how storms and their associated timing impact carbon cycling on the Scotian Shelf.

The study presented in this work largely rests on data from moored autonomous instruments such as the CARIOCA buoy, which supply observational data with high temporal coverage. The complementing use of SeaHorse data has expanded the observations into the vertical dimension, which facilitates the consideration of water column properties and their influence on the surface water CO_2 variability. In observational studies always a balance has to be found between temporal and spatial coverage, as for example discussed by Schiettecatte et al., (2007). The use of data from moored instruments evidently provides high temporal resolution data, needed to understand high-frequency variability. This strength of this study is at the expense of spatial coverage, which we have attempted to, at least partially, overcome, by using remotely sensed data such as temperature and Chl-a. However, we cannot fully exclude lateral processes, which might contribute to the variability of the CO_2 system as observed by our instruments.
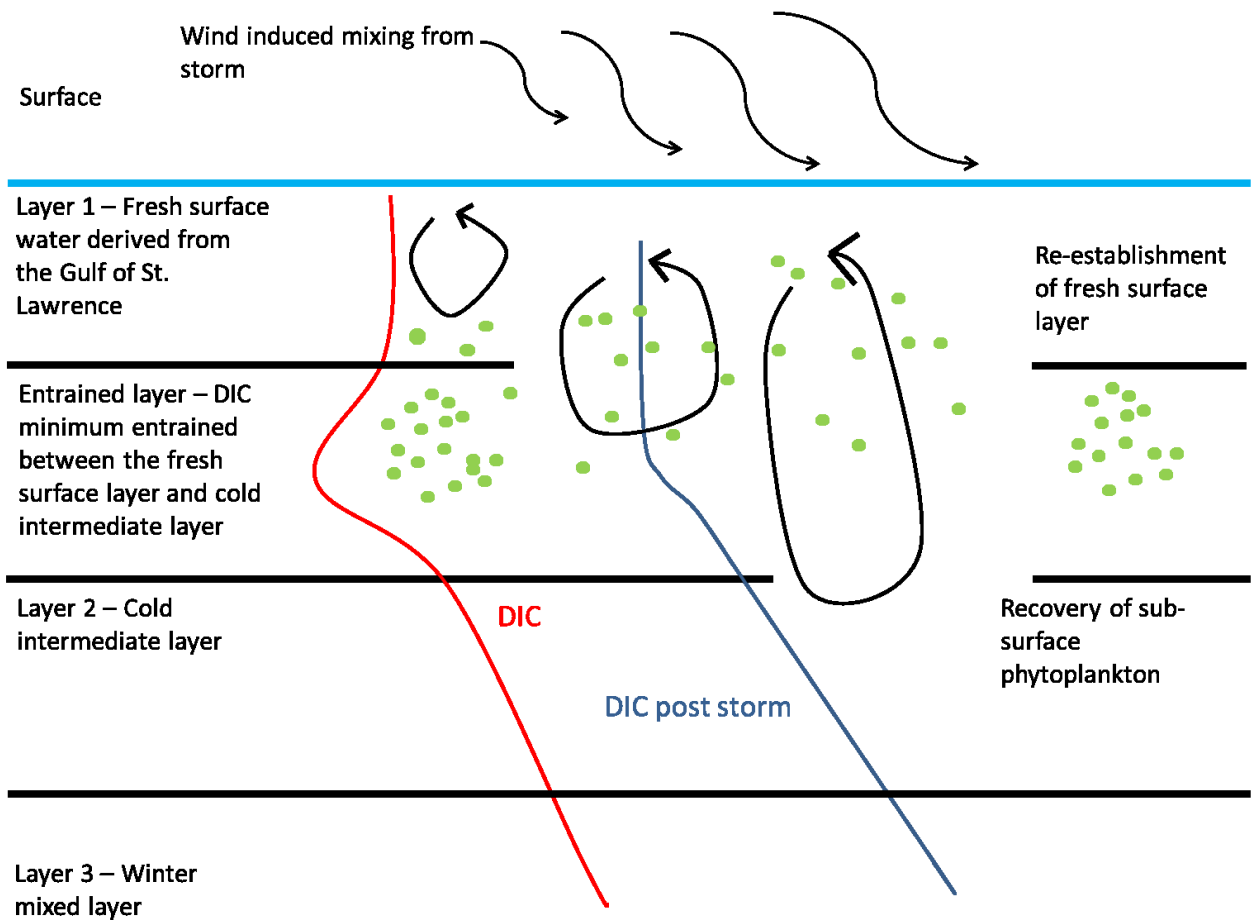
Figure 17: Schematic demonstrating the process of how storms alter the water column structure. Phytoplankton near the interface between layer 1 and 2 are brought to the surface through wind induced mixing. Once near the surface the increased light allows them to grow rapidly, using the nutrients that are also brought to the surface. If the storm is strong enough or persists for a while the third layer is also breached. This bring up the higher DIC waters, raising pCO_2, as expected prior to this study.

BIBLIOGRAPHY

Bakker, D.C.E., J. Etcheto, L. Merlivat, Variability of surface water fCO_2 during seasonal upwelling in the equatorial Atlantic Ocean as observed by a drifting buoy, *Geophys. Res.*, 106, 9241-9253, 2001.

Bates, N.R., M.H.P. Best, D.A. Hansell, Spatio-temporal distribution of dissolved inorganic carbon and net community production in the Chukchi and Beaufort Seas, *Deep Sea Res.*, 52, 3303-3323, 2005.

Bates, N.R., A.H. Knap, and A.F. Michaels, Contribution of hurricanes to local and global estimates of air-sea exchange of CO_2, *Nature*, 395, 58-61, 1998.

Bates, N.R. and L. Merlivat, The influence of short-term wind variability on air-sea CO_2 exchange, *Geophysical Research Letters*, 28(17), 3281-3284, 2001.

Bates, N.R., L. Merlivat, L. Beaumont, A.C. Pequignet, Intercomparison of shipboard and moored CARIOCA buoy seawater fCO_2 measurements in the Sargasso Sea, *Mar. Chem.*, 72, 239-255, 2000.

Bates, N.R., L. Samuels, L. Merlivat, Biogeochemical and physical factors influencing seawater fCO_2 and air-sea CO_2 exchange on the Bermuda coral reef, *Limnol. Oceanogr.*, 46, 833-846, 2001.

Borges, A.V., B. Delille, M. Frankignoulle, Budgeting sinks and sources of CO_2 in the coastal ocean: diversity of ecosystem counts*, Geophys. Res. Lett.*, 32, L14601, 2005.

Cai, W.J., Z.A. Wang, Y. Wang, The role of marsh-dominated heterotrophic continental margins in transport of CO_2 between the atmosphere, the land-sea interface and the ocean, *Geophys. Res. Lett.*, 30, 1849, 2003.

Chen-Tung, A.C. and A.V. Borges, Reconciling opposing views on carbon cycling in the coastal ocean: Continental shelves as sinks and near-shore ecosystems as sources of atmospheric CO_2, *Deep-Sea Research II*, 56, 578-590, 2009.

Cullen, J.J., Subsurface Chlorophyll maximum layers: enduring enigma or mystery solved? – *Annu. Rev. Mar. Sci.*, 7, 207-230, 2015.

Craig, S.E., H. Thomas, C.T. Jones, W.K.W. Li, B.J.W. Greenan, E.H. Shadwick, W.J. Burt, The effect of seasonality in phytoplankton community composition on CO_2 uptake on the Scotian Shelf, *J. Marine System*, 147, 52-60, 2015.

Crosswell, J.R., M.S. Wetz, B. Hales, and H.W. Paerl, Extensive CO_2 emissions from shallow coastal waters during passage of Hurricane Irene (August 2011) over the Mid-Atlantic Coast of the U.S.A., *Limnol. Oceanogr.*, 59(5), 1651-1665, 2014.

Dever, M., D. Hebert, B.J.W. Greenan, J. Sheng, P.C. Smith, Hydrography and Coastal Circulation along the Halifax Line and the Connections with the Gulf of St. Lawrence, *Atmosphere-Ocean*, 54:3, 199-217, 2016.

Fennel, K., J. Wilkin, M. Previdi, R. Najjar, Denitrification effects on air-sea CO2 flux in the coastal oceans: simulations for the Northwest North Atlantic, *Geophysical Research Letters*, 35, L24608, 2008.

Fennel, K., J. Wilkkin, J. Levin, J. Moisan, J. O'Reilly, D. Haidvogel, Nitrogen cycling in the Mid Atlantic Bight and implications for the North Atlantic nitrogen budget: Results from a three-dimensional model, *Global Biogeochemical Cycles*, 20, GB3007, 2006

Fuentes-Yaco, C., A.F. Vézina, M. Gosselin, Y. Gratton, P. Larouche, Influence of the late-summer storms on the horizontal variability of phytoplankton pigment determined by Coastal Zone Color Scanner images in the Gulf of St. Lawrence, Canada, *Ocean Optics XIII.* 2963, 678-683, 1997.

Fuentes-Yaco, C., E. Devred, S. Sathyendranath, T. Platt, Variation on surface temperature and phytoplankton biomass fields after the passage of hurricane Fabian in the western north Atlantic, *SPIE Symposium on Optics and Photonics, San Diego USA, July 31-August 4, 2005* 5885, 2005.

Fransson, A., M. Chierici, L.G. Anderson, I. Bussmann, G. Kattner, E.P. Jones, J.H. Swift, The importance of shelf processes for the modification of chemical constituents in the waters of the Eurasian Arctic Ocean: implications for carbon fluxes, *Cont. Shelf. Res.*, 21, 225-242, 2001.

Fratantoni, P.S. and R.S. Pickart, The western north Atlantic shelfbreak current system in summer, *Journal of Physical Oceanography*, 37, 2509-2533, 2007.

Friis, K., A. Körtzinger, D.W.R. Wallace, The salinity normalization of marine inorganic carbon chemistry data, *Geophysical Research Letters*, 30:2, 2003

GIOVANI satellite data available at: http://giovanni.gsfc.nasa.gov/giovanni/

Greenan, B. J.W., B.D. Petrie, W.G. Harrison, N.S. Oakey, Are the spring and fall blooms on the Scotian Shelf related to short-term physical events?, *Cont. Shelf. Res.*, 24, 603-625, 2004

Greenan, B. J.W., B.D. Petrie, W.G. Harrison, P.M. Strain, The onset and evolution of a spring bloom on the Scotian Shelf, *Limnol. Oceanogr.,* 53(5), 1759-1775, 2008.

Hood, E.M. and L. Merlivat, Annual to interannual variations of fCO2 in the northwestern Mediterranean Sea: results from hourly measurements made by CARIOCA buoys, 1995-1997, *J. Mar. Res.,* 59, 113-131, 2001.

Hood, E.M., L. Merlivat, and T. Johannessen, Variations of fCO_2 and air-sea flux of CO_2 in the Greenland Sea gyre using high-frequency time series data from CARIOCA drift buoys, *Journal of Geophysical Research*, 104, 20571-20583, 1999.

Huang, P. and J. Imberger, Variation of pCO_2 in ocean surface water in response to the passage of a hurricane, *Journal of Geophysical Research*, 115, C10024, 2010.

Johnson, K.M., K.D. Wills, D.B. Butler, W.K. Johnson, C.S. Wong, Coulometric total carbon dioxide analysis for marine studies: maximizing the performance of an automated gas extraction system and coulometric detector, Mar*. Chem.*, 44, 167-188, 1993.

Kiefer, D.A., Fluorescence properties of natural phytoplankton populations, Mar*. Biol.*, 22, 263-269, 1973.

Loder, J.W., G. Han, C.G. Hannah, D.A. Greenberg, P.C. Smith, Hydrography and baroclinic circulation in the Scotian Shelf region: winter versus summer, *J. Fish. Aquat. Sci.*, 54, 1997.

NOAA High Resolution SST data provided by the NOAA/OAR/ESRL PSD, Boulder, Colorado, USA, from their Web site at http://www.esrl.noaa.gov/psd/

Platt, T., H. Bouman, E. Devred, C. Fuentes-Yaco, S. Sathyendranath, Physical forcings and phytoplankton distributions, *Sci. Mar.* 69, 55-73, 2005

Shadwick, E.H., and H. Thomas,Seasonal and spatial variability in the CO_2 system on the Scotian Shelf (Northwest Atlantic), *Marine Chemistry*, 160, 42-55, 2014.

Shadwick, E.H., H. Thomas, A. Comeau, S.E. Craig, C.W. Hunt, J.E. Salisbury, Air-sea CO2 fluxes on the Scotian Shelf: Seasonal to multi-annual variability, *Biogeosciences*, 7, 3851-3867, 2010.

Shadwick, E.H., H. Thomas, K. Azetsu-Scott, B.J.W. Greenan, E. Head, E. Horne, Seasonal variability of dissolved inorganic carbon and surface water pCO2 in the Scotian Shelf region of the Northwest Atlantic , *Marine Chemistry*, 124, 23-37, 2011.

Signorini, S.R., A. Mannino, M. Friedrichs, R.G. Najjar, W.J. Cai, J. Salisbury, Z.A. Zhang, H. Thomas, E.H. Shadwick, Surface Ocean pCO_2 Seasonality and Sea-Air CO2 Flux

estimates for the North American East Coast, *J. Geophys. Research, Oceans*, 118, 1-22, 2013.

Smith, P.C., B. Petrie, C.R. Mann, Circulation, Variability, and Dynamics of the Scotian Shelf and Slope, *J.Fish. Res. Board Can.* 35, 1067-1083, 1978.

Takahashi, T., S.C., Sutherland, C. Sweeney, A. Poisson, N. Metzel, B. Tillbrook, N.R. Bates, R. Wanninkhof, R.A. Feely, C.L. Sabine, J. Olafsson, Y. Nojiri, Global air-sea CO_2 flux based on climatological surface ocean CO_2 and seasonal biological and temperature effects, *Deep Sea Res. II*, 49, 1601-1622, 2002.

Thomas, H., Y. Bozec, H.J.W. de Baar, K. Elkalay, M. Frankignoulle, L.S. Schiettecatte, G. Kattner, A.V. Borges, The carbon budget of the North Sea, *Biogeosciences*, 2, 87-96, 2005.

Thomas, H., S.E. Craig, B.J.W. Greenan, W.J. Burt,G. Herndl, S. Higginson, L. Salt, E.H. Shadwick, J.
Urrego Blanco, Directs observations of diel biological CO_2 fixation on the Scotian Shelf, Northwestern Atlantic Ocean, *Biogeosciences*, 9, 2301-2309, 2012.

Thomas, H., L.S. Schiettecatte, K. Suykens, Y. J.M. Koné, E.H. Shadwick, A.E.F. Prowe, Y. Bozec, H. J.W. de Baar, A.V. Borges, Enhanced ocean carbon storage from anaerobic alkalinity generation in coastal sediments, *Biogeosciences*, 6, 267-274, 2009.

Urrego-Blanco, J. and J. Sheng, Interannual variability of the circulation over the Easter Canadian Shelf, *Atmosphere-ocean*, 50(3), 277-300, 2012.

Vandemark, D., J.E. Salisbury, C.W. Hunt, S.M. Shellito, J.D. Irish, W.R. McGillis, C.L. Sabine, S.M. Maenner, Temporal and spatial dynamics of CO_2 air-sea flux in the Gulf of Maine, *Journal of Geophysical Research*, 116, 1-4, 2011.

Walker, N.D., R.R. Leben, and S. Balasubramanian, Hurricane-forced upwelling and chlorophyll a enhancement within cold-core cyclones in the Gulf of Mexico, *Geophysical Research Letters*, 32, L18610, 2005.

Wanninkhof, R., Relationship between wind speed and gas exchange over the ocean revisited, *Limnol. Oceanogr.: Methods*, 12, 351-362, 2014.

Walsh, J.J., Importance of continental margins in the marine biogeochemical cycling of carbon and nitrogen, *Nature*, 350, 753-755, 1991.